COMPOSITIO MATHEMATICA

The space of solvable Pell–Abel equations

Andrei Bogatyrëv and Quentin Gendron

Compositio Math. **161** (2025), 1483–1511.

doi: 10.1112/S0010437X25007158

FOUNDATION
COMPOSITIO
MATHEMATICA



LONDON
MATHEMATICAL
SOCIETY
EST. 1865



https://doi.org/10.1112/S0010437X25007158 Published online by Cambridge University Press

Compositio Math. 161 (2025) 1483–1511
doi:10.1112/S0010437X25007158

The space of solvable Pell–Abel equations

Andrei Bogatyrëv and Quentin Gendron

To the memory of Igor Moiseevich Krichever.

Abstract

A Pell–Abel equation is a functional equation of the form $P^2 - DQ^2 = 1$, with a given polynomial D free of squares and unknown polynomials P and Q. We show that the space of Pell–Abel equations with the degrees of D and of the primitive solution P fixed is a complex manifold. We describe its connected components by an efficiently computable invariant. Moreover, we give various applications of this result, including to torsion pairs on hyperelliptic curves and to Hurwitz spaces, and a description of the connected components of the space of primitive k-differentials with a unique zero on genus 2 Riemann surfaces.

1. Introduction

The reincarnation of Pell's Diophantine equation in the realm of polynomials was introduced and investigated by Abel in [Abe26]. Since then, the equation

$$P^2(x) - D(x)Q^2(x) = 1 \tag{PA}$$

has been known as the *Pell–Abel equation*. Here, $P(x)$ and $Q(x)$ are unknown polynomials of one variable and $D(x) := \prod_{e\in\mathsf{E}}(x-e)$ is a monic complex polynomial of given degree $\deg D = |\mathsf{E}| := 2g+2$ without multiple roots. For a generic choice of D, the Pell–Abel equation only admits the trivial solutions $(P,Q) = (\pm 1, 0)$. If an equation has a nontrivial solution, then the set of solutions is infinite and contains a unique, up to sign, polynomial with minimal degree $n := \deg P > 0$. This solution is called *primitive*. It generates the other solutions P via composition with the classical Chebyshev polynomials and a change of sign. This is discussed in more detail in § 2.

Let us fix $g \geqslant 0$ and $n \geqslant 1$ and consider the set $\tilde{\mathscr{A}}_g^n$ of monic polynomials D of degree equal to $2g+2$ whose associated Pell–Abel equations have a primitive solution of degree n. The affine group $x \mapsto ax+b$ with $a \in \mathbb{C}^*$ and $b \in \mathbb{C}$ acts on the set of monic polynomials as $D(x) \mapsto a^{-\deg D} D(ax+b)$. This action does not affect the degree n of the primitive solution of (PA). Our main object of study is the quotient $\mathscr{A}_g^n$ of the set $\tilde{\mathscr{A}}_g^n$ by this group action. More precisely, we have the following result, which is proved in § 3.

Received 19 June 2023, accepted in final form 6 January 2025, published online 1 September 2025.
2020 Mathematics Subject Classification 32G13 (primary), 30C10, 30F30, 14H15, 14H45 (secondary).
Keywords: Pell-Abel equation; polynomial Pell equation; hyperelliptic Riemann surfaces; isoperiodic leaves; k-differentials; Hurwitz spaces; torsion points.
© The Author(s), 2025. This is an Open Access article, distributed under the terms of the Creative Commons Attribution licence (https://creativecommons.org/licenses/by/4.0/), which permits unrestricted re-use, distribution, and reproduction in any medium, provided the original work is properly cited. *Compositio Mathematica* is © Foundation Compositio Mathematica.

https://doi.org/10.1112/S0010437X25007158 Published online by Cambridge University Press

Theorem 1.1. *The set $\tilde{\mathscr{A}}_g^n$ is invariant under the action of the affine group. The quotient $\mathscr{A}_g^n$ is a smooth orbifold of complex dimension g.*

An introduction to orbifolds can be found in [Thu79, § 13], and in the first approximation we can think of them as manifolds.

The main result of this paper consists in the classification of the connected components of the spaces $\mathscr{A}_g^n$. A weaker version was announced in [BG23], which contains a survey of the proof given below.

We first introduce the *degree partition invariant* of an element $D \in \mathscr{A}_g^n$. Given a primitive solution P of (PA), its value $P(e) = \pm 1$ at any zero $e \in \mathsf{E}$ of D. Therefore the set E can be decomposed into two subsets $\mathsf{E}^{\pm}$ and we obtain the partition of the degree of D:

$$|\mathsf{E}| = 2g + 2 = |\mathsf{E}^+| + |\mathsf{E}^-|.$$

The choice of the other primitive solution $-P$ interchanges the indexes $\pm$ in the summands, but the unordered partition remains the same. The *degree partition invariant* of D is the unordered pair of nonnegative integers $(|\mathsf{E}^-|, |\mathsf{E}^+|)$.

Theorem 1.2. *Let $m = \min(g, n-g-1)$ and let $[\cdot]$ denote the integer part. Equation (PA) has no primitive solutions of degree $n < g+1$ or $n > 1$ when $g = 0$. Otherwise, the number of components $a(g,n)$ of $\mathscr{A}_g^n$ is equal to $[m/2]+1$ if $n+g$ is odd and $[(m+1)/2]$ if $n+g$ is even. Moreover, each component is labelled by a unique degree partition $(|\mathsf{E}^-|, |\mathsf{E}^+|)$ satisfying:*

(1) $|\mathsf{E}^{\pm}| > 0$;
(2) $|\mathsf{E}^{\pm}| \leqslant n$; *and*
(3) *the parity of $|\mathsf{E}^{\pm}|$ is equal to the parity of n.*

This theorem has two trivial cases. When $n < g+1$, the degree of P^2 is strictly less than the degree of DQ^2 if the solution (P,Q) is not trivial. When $g = 0$, any (PA) is brought to the case $D(x) = x^2 - 1$ by a linear change of variable, and admits the (primitive) solution $(P,Q) = (x,1)$ of degree $n = 1$. All the other cases are far less trivial. They are based on a pictorial calculus representing the flat structure on the Riemann surface that we associate with each Pell–Abel equation.

First, in § 2, we associate, with every (marked) hyperelliptic Riemann surface, a distinguished abelian differential. Using this, we propose a solvability criterion for the Pell–Abel equation in terms of the periods of this differential. Then, in § 4, we explain the graphical technique which allows us to control the periods of the distinguished differential when we deform the polynomial D. The upper bound for the number of connected components is obtained in § 5, where we bring the graph of an arbitrary solvable Pell–Abel equation to one of the standard forms. Finally, we discuss the degree partition invariant in § 6. We show that this invariant appears in the context of braids, and that all standard forms have different invariants and hence lie in different components.

1.1 Applications

The Pell–Abel equation is inherently connected to many problems in different branches of mathematics. To cite some of these, it appears in the reduction of abelian integrals [Abe26, Che48, BE01], Poncelet's porism [BZ13], elliptic billiards [DR19], approximation theory [SY92, Peh93, Bog12, Bog02], spectral theory for infinite Jacobi matrices [SY92], algebraic geometry including the study of Frobenius endomorphisms [Ser19], complex affine surfaces [Kol20], and Teichmüller curves [McM06].

https://doi.org/10.1112/S0010437X25007158 Published online by Cambridge University Press

We now give some examples of where our main result may be directly translated or applied.

1.1.1 *Extremal polynomials.* Shabat polynomials, meaning polynomials with just two finite critical values, are rigid objects, but many applications require maps with similar properties that are more flexible. These polynomials were defined in [Bog02, Bog12] under the name of *g-extremal polynomials* and in [Zan14, § 12.2.2] or [BCZ22, § 2] as *almost-Belyi maps*. A typical g-extremal polynomial $P(x)$ has only simple critical points, with almost all critical values equal to ± 1 and exactly g exceptional critical values not lying in this set. In general we allow the critical points to be merged, and the extremality weight g defined, for example, in [Bog02, Bog12] takes into account the confluent critical points, even if the appropriate critical value lies in the exceptional set $\{\pm 1\}$.

The practical interest in g-extremal polynomials comes from some problems of uniform Chebyshev optimization: the vast majority of the alternation points that arise for the solution will be the critical ones that have values in the two-element set: $\pm$ the value of the approximation error. After re-normalization they become g-extremal with some small value of the parameter g. Classical examples are Chebyshev and Zolotarev polynomials for $g = 0$ and $g = 1$, respectively.

Any polynomial P is a solution of the unique Pell–Abel equation: just extract the square-free part D in the polynomial $P^2 - 1$. A simple calculation (see [Bog02, § 3]) shows that $\deg D = 2g + 2$ where g is the extremality number of the polynomial P. The set of g-extremal complex polynomials of given degree $N \geqslant g + 1$ is a smooth complex manifold of dimension $g + 2$, and the number of its components may be counted with the use of our main theorem. Indeed, every g-extremal polynomial $P_N(x)$, as a solution of a Pell–Abel equation, has a unique representation of the kind $\pm T_m \circ P_n(x)$, where T_m is the classical degree m Chebyshev polynomial and P_n is the primitive solution of the same Pell–Abel equation (see Theorem 2.1). One can show that the inverse polynomials $\pm P_N$ lie in the same component of the set of g-extremal polynomials exactly when the corresponding degree partition has equal parts: $|\mathsf{E}^{\pm}| = g + 1$. Eventually, we arrive at following corollary.

Corollary 1. *The deformation space of g-extremal polynomials of a given degree N consists of one or two components when $g = 0$ and N is, respectively, odd or even. For $g > 0$ the same number is equal to*

$$\sum_{n|N} 2a(g,n) - \#\left\{ n \in \mathbb{N} : \frac{N}{n} \text{ is odd and } n - g = 1, 3, 5, \dots \right\}, \tag{1}$$

where $a(g,n)$ is the number of components of $\mathscr{A}_g^n$.

1.1.2 *Hurwitz spaces.* A typical g-extremal polynomial of degree N with different exceptional critical values gives us a covering of a sphere by another sphere which is branched in a specific way. The cyclic type of monodromy above $g + 2$ finite critical points is described by the following passport (see [LZ04] for definitions):

$$[2^A 1^{N-2A};\ 2^B 1^{N-2B};\ g \times 2^1 1^{N-2}]$$

with integers $2 \leqslant A, B \leqslant N/2$ satisfying the planarity (or Riemann–Hurwitz) condition

$$A + B + g = N - 1.$$

Again, the polynomials P_N that realize the above passport after their re-normalization have a representation as the composition of a classical Chebyshev polynomial T_m and a primitive solution P_n of some Pell–Abel equation. We should distinguish between two cases: for even m,

https://doi.org/10.1112/S0010437X25007158 Published online by Cambridge University Press

the maximum of $2A, 2B$ is equal to N and the minimum is equal to $N-2g-2$; for odd m, the positive numbers $N-2A$ and $N-2B$ make up the degree partition for P_n.

Corollary 2. *The Hurwitz space of degree N polynomials with the above monodromy passport has the following number of components:*

(1) *the number of the integer n such that N/n is odd and $n \geqslant N-2\min(A,B)$, when the degree $N > 2\max(A,B)$*; and
(2) *the sum $\sum_n a(g,n)$ over integers n such that N/n is even, when $N = 2\max(A,B)$.*

Note that this result generalizes works with similar passports in [Waj96, LO08, MP18] and partial results on these passports in [KZ96] and in [LZ04, Table 5.1]. Moreover, the use of abelian differentials to study Hurwitz spaces appeared previously in [Mul22].

1.1.3 *Torsion points.* Given a genus g hyperelliptic Riemann surface M with hyperelliptic involution J and a non-Weierstraß marked point p, we can ask when the Abel–Jacobi image of the divisor $p - Jp$ has some finite order n in the Jacobian. Equivalently, we can ask about the existence of a function $f \in \mathbb{C}(M)$ whose divisor is $n(p-Jp)$. This problem is equivalent to the solvability of some Pell–Abel equation, which we explain in Remark 1 of § 2. Therefore, we make the following claim.

Corollary 3. *The number of connected components of the space of hyperelliptic Riemann surfaces M of genus g with a primitive n-torsion pair of points conjugated by the hyperelliptic involution is equal to $a(g,n)$. The degree partition $(|\mathsf{E}^-|, |\mathsf{E}^+|)$ is the number of $e \in \mathsf{E}$ such that $f(e,0) = \pm 1$ for a suitable normalization of this function in the algebraic model (2) of $M = M(\mathsf{E})$.*

1.1.4 *Strata of k-differentials.* A more elaborate application is the following result, which is proved in § 7 (where the basic definitions are recalled).

Corollary 4. *The moduli space of primitive k-differentials with a unique zero of order $2k$ on genus 2 Riemann surfaces $\Omega^k\mathcal{M}_2(2k)^{\mathrm{prim}}$ is empty for $k=2$, connected for $k=1,3$ or $k \geqslant 4$ and even, and has two connected components for $k \geqslant 5$ and odd. Moreover, the component of $\mathscr{A}_2^n$ of degree partition invariant $(1,5)$, respectively $(3,3)$, corresponds to the component of odd, respectively even, parity of the strata $\Omega^k\mathcal{M}_2(2k)^{\mathrm{prim}}$.*

The proof of the second part of the corollary is given in Proposition 7.2 by considering the torsion packets modulo the Weierstraß points, which may be of independent interest.

2. Solvability of Pell–Abel equation

Fix a polynomial D of degree $2g+2$ whose roots are all simple. The union of these roots is denoted by E. Some conditions on D have to be imposed [Abe26, Che48, Mal02, SY92] to guarantee the existence of a nontrivial solution of the Pell–Abel equation (PA), that is with $n := \deg P > 0$. The criterion given by Abel is the periodicity of the continued fraction for the square root of D (see [Pla14] and the references therein for a more modern presentation). We will use a transcendental criterion coming from [Bog02, Bog12] which is much easier to handle.

We associate, with the polynomial $D(x) = \prod_{e\in\mathsf{E}}(x-e)$, the affine genus g hyperelliptic Riemann surface

$$M = M(\mathsf{E}) := \left\{(x,w) \in \mathbb{C}^2 : w^2 = D(x)\right\}. \tag{2}$$

https://doi.org/10.1112/S0010437X25007158 Published online by Cambridge University Press

The latter admits the natural two-point compactification

$$M_\infty := M \cup \{\infty_\pm\} \tag{3}$$

where the points $\infty_\pm$ are distinguished by the limit value of the function $w^{-1}x^{g+1}(\infty_\pm) = \pm 1$. The added points are interchanged by the hyperelliptic involution $J(x,w) = (x,-w)$ acting on M_∞. In what follows, we will suppose that the points $\infty_\pm$ are marked on the Riemann surface M_∞.

The Riemann surface M_∞ associated with D bears a unique meromorphic differential of the third kind,

$$d\eta = d\eta_M = (x^g + a_{g-1}x^{g-1} + \cdots + a_0)w^{-1}\,dx, \tag{4}$$

having two simple poles at infinity with residues $\operatorname{Res} d\eta|_{\infty_\pm} := \mp 1$ and purely imaginary periods (see [GK10, Proposition 3.4]). This differential will be referred to as the *distinguished differential*.

Note that the distinguished differential is odd with respect to hyperelliptic involution, that is, it satisfies $J^*d\eta = -d\eta$. In particular, the quadratic differential $(d\eta)^2$ descends to the Riemann sphere so that $d\eta$ is the canonical cover of $(d\eta)^2$ in the terminology of [BCG+19]. This quadratic differential is referred to as the *distinguished quadratic differential*.

We give the criterion for the solvability of (PA) in terms of the distinguished differential.

Theorem 2.1. *Given $n \geqslant 1$, (PA) admits a nontrivial solution with $\deg P = n$ if and only if all the periods of $d\eta_M$ on M are contained in the lattice $2\pi i\mathbb{Z}/n$.*

If this condition is satisfied, then the solution of the Pell–Abel equation is given, up to sign, by

$$P(x) = \cos\left(ni\int_{(e,0)}^{(x,w)} d\eta_M\right) \quad \text{and} \quad Q(x) = iw^{-1}\sin\left(ni\int_{(e,0)}^{(x,w)} d\eta_M\right). \tag{5}$$

Proof. If (PA) has a nontrivial solution (P,Q) then the (Akhiezer) rational function $f(x,w) = P(x) + wQ(x) \in \mathbb{C}(M_\infty)$ satisfies $f(x,-w) = 1/f(x,w)$. Hence it has a unique pole at ∞_+ and a unique zero at ∞_-, both of multiplicity n. In that case, the distinguished differential is equal to $d\eta = n^{-1}d\log(f(x,w))$. The fact that log is a multi-valued function implies that the periods of $d\eta$ lie in $2i\pi\mathbb{Z}/n$.

Conversely, the lattice condition

$$\int_{H_1(M,\mathbb{Z})} d\eta_M \subset 2\pi i\mathbb{Z}/n \tag{6}$$

and the fact that $J^*d\eta = -d\eta$ imply that the functions on the right-hand sides of Equation (5) are polynomials of degree n and $n-g-1$ respectively. Now the classical Pythagorean theorem $\sin^2(z) + \cos^2(z) = 1$ for $z \in \mathbb{C}$ reads as the Pell–Abel equation. □

Remark 1.

(1) The lattice condition as the criterion for the solvability of the Pell–Abel equation seems to have first appeared in approximation theory and is related to the Chebyshev approach to least deviation problems [Zol77, Bog12]. Some particular cases may be found in [Rob64, SY92, Peh93, Bog99, Bog02].

(2) Given a polynomial D, the set of all solutions of (PA) admits a group structure which mimics the multiplication of Akhiezer functions:

$$(P,Q) * (p,q) = (Pp + DQq, Pq + Qp). \tag{7}$$

https://doi.org/10.1112/S0010437X25007158 Published online by Cambridge University Press

The trivial solution $(1,0)$ is the unit of this group, and the inverse of (P,Q) is $(P,-Q)$. It follows from the trigonometric representation of the solutions given in (5) that the primitive solution generates all higher degree solutions via composition with the classical Chebyshev polynomial and possibly a change of sign.

(3) Note that if (PA) has a nontrivial solution (P,Q) of degree n, then the Akhiezer function $f(x,w)=P(x)+wQ(x)\in\mathbb{C}(M_\infty)$ has divisor $n\infty_+-n\infty_-$. This means that the divisor $\infty_+-\infty_-$ is of primitive n-torsion if and only if (PA) has a primitive solution of degree n. Corollary 3 follows readily from Theorem 1.2 using this remark.

3. Space of Pell–Abel equations

Let us study the constraints imposed by the lattice condition (6) of Theorem 2.1. Consider the space $\tilde{\mathcal{H}}_g$ of complex monic square-free polynomials $D(x)$ of degree $2g+2$. This may be identified with the space $\mathbb{C}^{2g+2}$ with a removed discriminant set. The disjoint zeros $e\in\mathsf{E}$ may serve as local coordinates of this complex manifold. The polynomials such that the Pell–Abel equation (PA) has a *primitive* solution of degree $n\geqslant 1$ form a subset $\tilde{\mathscr{A}}_g^n$ of $\tilde{\mathcal{H}}_g$. We show that this subset is a manifold.

Theorem 3.1. *The set of polynomials $\tilde{\mathscr{A}}_g^n$ is either empty or a smooth complex manifold of pure dimension $g+2$.*

The proof relies on the fact that the set $\tilde{\mathscr{A}}_g^n$ is given by the polynomials $D(x)$ such that the associated distinguished differential $d\eta$ on M satisfies the lattice condition (6) of Theorem 2.1.

Proof. Consider the space of non-normalized abelian differentials

$$d\eta(\mathsf{B},\mathsf{E}):=\frac{(x^g+\sum_{s=0}^{g-1}b_sx^s)}{\sqrt{\prod_{j=1}^{2g+2}(x-e_j)}}\,dx,$$

with coordinates $(\mathsf{B},\mathsf{E}):=(b_0,\dots,b_{g-1};e_1,\dots,e_{2g+2})$. Note that this is a natural fibration over the space $\tilde{\mathcal{H}}_g$.

Let us fix $2g+1$ closed paths on the given twice-punctured surface $M=M(\mathsf{E}_0)$ which represent a basis of the homology group $H_1(M,\mathbb{Z})$ (an extra nontrivial cycle encompasses a puncture). By deforming the loops within their homology class we suppose that the projections $C_0,C_1,\dots,C_{2g}$ of those contours to the x-plane are disjoint from the branching set E_0. Therefore for all $\mathsf{E}\in\tilde{\mathcal{H}}_g$ in a small vicinity of E_0 the lifts of those contours to the surface $M(\mathsf{E})$ represent the basis of the first homology group. We denote by C_0 the cycle encompassing a puncture at infinity.

We also fix $g+2$ paths D_s on the complex plane disjoint from the branching set E_0, starting at a common point p_0 and ending at arbitrarily chosen but distinct points p_s, for $s=1,\dots,g+2$. Finally, we fix a loop D_0 lifting to an open path on $M(\mathsf{E}_0)$ and connecting two preimages of p_0 on the surface. This set of data provides us with $3g+2$ locally defined holomorphic functions:

$$\pi_j(\mathsf{B},\mathsf{E}):=\int_{C_j}d\eta(\mathsf{B},\mathsf{E})\quad\text{for } j=1,2,\dots,2g,$$
$$\tau_s(\mathsf{B},\mathsf{E}):=\int_{D_s}d\eta(\mathsf{B},\mathsf{E})+\frac{1}{2}\int_{D_0}d\eta(\mathsf{B},\mathsf{E})\quad\text{for } s=1,2,\dots,g+2.$$

If the coordinate change $(\mathsf{B},\mathsf{E})\to(\pi,\tau)$ is degenerate at the point $(\mathsf{B}_0,\mathsf{E}_0)$, there exists a tangent vector $\sum_j\beta_j(\partial/\partial b_j)+\sum_s\epsilon_s(\partial/\partial e_s)$ annihilating all these functions at this point of the

https://doi.org/10.1112/S0010437X25007158 Published online by Cambridge University Press

space of differentials. This means that the differential

$$d\zeta := \frac{1}{2}\sum_{s=1}^{2g+2}\epsilon_s\frac{d\eta_M}{x-e_s} + \sum_{j=0}^{g-1}\beta_j\frac{x^j dx}{w}$$

determined by the tangent vector satisfies the equations

$$\int_{C_s} d\zeta = 0 \quad \text{for all } s = 1,\dots,2g,$$
$$\left(\int_{D_j} + \frac{1}{2}\int_{D_0}\right) d\zeta = 0 \quad \text{for all } j = 1,\dots,g+2.$$

All the periods of the $d\zeta$, both polar and cyclic, vanish and therefore its integral is a single valued function on the surface $M(\mathsf{E}_0)$:

$$\zeta(P) := \frac{1}{2}\left(\int_{P_0}^{P} + \int_{JP_0}^{P}\right) d\zeta \quad \text{with } \zeta(P_0) = p_0. \tag{8}$$

The differential $d\zeta$ is odd with respect to the hyperelliptic involution J, and so is its integral $\zeta(P)$ for the chosen constant of integration. The only possible singularities of the meromorphic function $\zeta(P)$ are simple poles at the branchpoints of M whose number is not greater than $2g+2$. It is strictly less than the $2g+4$ zeros of $\zeta(P)$, which cover all the endpoints $x = p_s$ of the integration paths D_s in the formulas above. Hence $d\zeta$, and therefore the annihilating tangent vector, vanish.

We conclude that the set locally defined by fixing the values of all periods of the differential $d\eta(\mathsf{B},\mathsf{E})$ is a smooth complex analytic manifold of dimension $g+2$ in the fibration over the space $\tilde{\mathcal{H}}_g$. It remains to show that it does not degenerate under the projection to the base $\tilde{\mathcal{H}}_g$. If the isoperiodic manifold had two points gluing under the projection, or a vertical tangent, this would mean the existence of a non-zero holomorphic differential with vanishing periods. The latter is prohibited by the Riemann bilinear relations. □

Remark 2. The counterpart of this theorem for real curves was proved in [Bog12, Chapter 5].

Note that isoperiodic (or Pell–Abel) manifolds $\tilde{\mathscr{A}}_g^n$ are invariant under the action of the one-dimensional affine group $\mathsf{E} \to a\mathsf{E} + b$ with $(a,b) \in \mathbb{C}^* \times \mathbb{C}$. Indeed, this transformation does not change the conformal structure on the Riemann surface with the marked point at infinity. Hence, the distinguished differential and all its periods survive under this map.

Corollary 5. *The quotient $\mathscr{A}_g^n$ of $\tilde{\mathscr{A}}_g^n$ by the action of the affine group is a smooth orbifold of complex dimension g.*

Proof. This follows directly from Theorem 3.1 and the fact that the action of the affine group on any set of $2g+2$ points in the plane has finite stabilizer. □

4. Pictorial representation

In this section we introduce a pictorial representation of the moduli space of hyperelliptic Riemann surfaces M_∞ carrying a couple of marked points $\infty_\pm$ conjugated by the hyperelliptic involution. We associate with such a Riemann surface the planar graph whose edges are critical leaves of the vertical and horizontal foliations of the distinguished quadratic differential $(d\eta_M)^2$ introduced in § 2. We will completely characterize the graphs of this type, and each of them will come from a unique, up to the action of the affine group, pointed Riemann surface M_∞.

https://doi.org/10.1112/S0010437X25007158 Published online by Cambridge University Press

Originally this graphic language was used in [Bog03, Bog12] for the theory of real extremal polynomials, where the problem of the deformation of Riemann surfaces with control of the periods also exists. It turned out to be very useful in the investigation of the global periods map, particularly for its image [Bog03] and the study of the topology of its fibres [Bog19].

4.1 Global width function

Let M_∞ be a hyperelliptic Riemann surface with marked points $\infty_\pm$, and $d\eta$ be its distinguished differential. Given a branchpoint $e \in \mathsf{E}$, we define the *width function* $W : \mathbb{C} \to \mathbb{R}_+$ by

$$W(x) = \left| \operatorname{Re} \int_{(e,0)}^{(x,w)} d\eta \right|. \tag{9}$$

One can immediately check that the normalization conditions of the distinguished differential imply that the width function satisfies the following properties:

(1) W is a well-defined single-valued function on the plane;
(2) W is harmonic outside its zero set $\Gamma_{\mathsf{I}} := \{x \in \mathbb{C} : W(x) = 0\}$;
(3) W has a logarithmic pole at infinity;
(4) W vanishes at each branchpoint $e' \in \mathsf{E}$.

We only comment on property (4). Since $d\eta$ is odd with respect to hyperelliptic involution, the value $W(e')$ is equal to one half of the modulus of the real part of some period of $d\eta$. Since all its periods are purely imaginary, this gives (4). Moreover, this implies that the width function is independent of the choice of the branchpoint e as the initial point of integration.

4.2 Construction of the associated graph $\Gamma(M)$.

Recall that a quadratic differential induces a vertical and a horizontal foliation (see [Str84] for a detailed discussion). The level lines of the width function are the trajectories of the vertical foliation of the distinguished quadratic differential $(d\eta)^2$, while the steepest descent lines of $W(x)$ are its horizontal trajectories.

We associate, with any Riemann surface M, a weighted *planar* graph $\Gamma = \Gamma(M)$ which is a union of a 'vertical' subgraph Γ_{I} and a 'horizontal' subgraph $\Gamma_{\mathsf{_}}$. The precise definition is given below, and examples of such graphs are given in Figure 1.

Definition 4.1. Let M be the hyperelliptic Riemann surface given by Equation (2). Its associated graph $\Gamma(M)$ is the weighted planar graph constructed as follows.

– The vertical edges are the unoriented arcs of the zero set of $W(x)$ (they are segments of the vertical foliation of $(d\eta)^2$).
– The horizontal edges are the segments of the horizontal foliation of $(d\eta)^2$ connecting saddle points of the function W to the zero level set of W (which may occasionally hit other saddle points on its path). The horizontal edges are oriented with respect to the growth of $W(x)$.
– The vertices of the graph Γ are the union of the finite points of the divisor of $(d\eta)^2$ and the points in $\Gamma_{\mathsf{I}} \cap \Gamma_{\mathsf{_}}$, i.e. projections of the saddle points of W to its zero set along the horizontal leaves.
– Each edge R of the graph is equipped with its length $h(R)$ in the metric $ds := |d\eta|$ induced by $(d\eta)^2$.

https://doi.org/10.1112/S0010437X25007158 Published online by Cambridge University Press

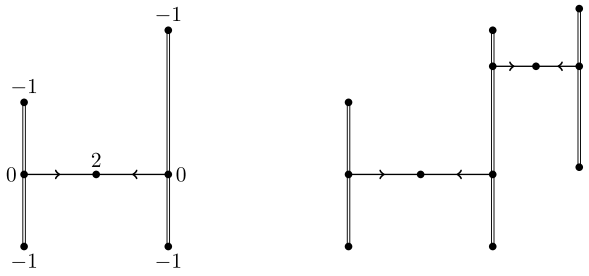


Figure 1. Typical graphs associated with Riemann surfaces of genera 1 and 2 are shown without their weights. For every vertex V of the first graph, the value of $\mathrm{ord}(V)$ is given.

Convention 4.2. In the figures, we draw the vertical edges of the canonical graph with double lines. The horizontal edges are represented by single lines with an arrow showing their orientation. The weight of a vertical edge R is denoted by $h(R)$. We do not usually put the values of the horizontal weights on the figures.

From the local behaviour of the trajectories one can immediately check that, for any vertex $V \in \Gamma$, its multiplicity in the divisor of $(d\eta)^2$ is given by

$$\mathrm{ord}(V) := d_{\mathbf{|}}(V) + 2d_{in}(V) - 2, \tag{10}$$

where $d_{\mathbf{|}}$ is the degree of the vertex with respect to the vertical edges and d_{in} is the number of incoming horizontal edges. The fixed points of the hyperelliptic involution of M correspond to the vertices V with the odd value of $\mathrm{ord}(V)$, and automatically lie on the vertical part of the graph Γ. One can check this statement for the graphs represented in Figure 1.

4.3 Admissible graphs

The graphs $\Gamma(M)$ associated with the hyperelliptic Riemann surfaces by the previous construction can be described in an axiomatic way. There are five conditions, three on the topology of the graph (T) and two on its weights (W).

Theorem 4.3. *A weighted planar graph Γ, considered as a topological object (up to isotopy of the plane), is associated with a hyperelliptic Riemann surface M if and only if the following five conditions are satisfied.*

(T1) *The graph Γ is a tree.*

(T2) *The horizontal edges leaving the same vertex are separated by a vertical or an incoming edge.*

(T3) *If $\mathrm{ord}(V) = 0$ then $V \in \Gamma_{\mathbf{_}} \cap \Gamma_{\mathbf{|}}$.*

(W1) *The width function increases along oriented edges, and $W(V) = 0$ if V lies on the vertical part of the graph.*

(W2) *The weights of the vertical edges are positive and their total sum is π.*

Given a graph Γ satisfying all five conditions, the Riemann surface M whose associated graph is Γ is unique up to the action of the linear maps $\mathrm{Aff}(1, \mathbb{C})$ on the branching set E.

Remark 3. These conditions imply some basic restrictions on the graphs $\Gamma(M)$. For instance, there are no pendent horizontal edges like ⟶• or •⟵. The first case is prohibited by (T2), while the second is prohibited by (T3).

https://doi.org/10.1112/S0010437X25007158 Published online by Cambridge University Press

Proof. We give a sketch of the proof for completeness, and the reader can look at [Bog03, Bog12] for a more detailed description.

Constraints on associated graph. We say a few words about the genesis of properties (T1), (T2), and (W2). Properties (T3) and (W1) follow directly from the definition of the graph Γ.

Property (T1). Suppose that the complement $\mathbb{C} \setminus \Gamma(M)$ of the graph is not connected. Let us calculate the Dirichlet integral of the width function in a bounded component Ω of the complement by means of Green's formula:

$$\int_\Omega |\operatorname{grad} W(x)|^2 \, d\Omega = \int_{\partial\Omega} W(x) \frac{\partial W}{\partial n} \, ds.$$

The function W vanishes on the vertical parts of the boundary, while its normal derivative vanishes at the horizontal parts of $\partial\Omega$. This would imply that W is constant. Now suppose that the graph has several components. Summing up the values of $\operatorname{ord}(V)$ over all its vertices, we get, by (10), that

$$2\sharp\{\text{vertical edges}\} + 2\sharp\{\text{horizontal edges}\} - 2\sharp\{\text{vertices}\} = -2\sharp\{\text{components of } \Gamma\}.$$

This value equals the degree of the divisor of $(d\eta_M)^2$ on the sphere (i.e. -4) plus the order of its pole at infinity (i.e. 2). Hence, the graph Γ has just one component and it is a single tree.

Property (T2). Let V be a vertex of Γ such that $W(V) > 0$. This is a saddle point of the width function, the meeting point of several alternating 'ridges' and 'valleys'. A horizontal edge comes into V from each valley, by definition. The outgoing edge (if any) goes along the ridge, so any two of them are separated. The same is true for $W(V) = 0$ with the vertical edges coming from each 'valley'.

Property (W2). The integral of $(d\eta)^2$ along the boundary of the plane cut along $\Gamma_{\mathbf{I}}$ equals $2i$ times the sum of the weights of all vertical edges. The integration path may be contracted to the path encompassing the pole at infinity, and hence by the residue theorem is $2i\pi$.

From the graph to the Riemann surface. The Riemann surface M may be glued from a finite number of strips in a way determined by combinatorics and the weights of the graph. We briefly describe the procedure below.

Given a planar graph satisfying the above five conditions, we extend it by drawing $d_{\mathbf{I}}(V) - d_{\text{out}}(V) + d_{\text{in}}(V) \geqslant 0$ outgoing horizontal arcs which connect each vertex V to infinity and are disjoint except possibly at their endpoints. For each vertex, we require that all the outgoing edges of this *extended graph* $\operatorname{Ext}\Gamma$, old and new, alternate with the incident edges of other types, incoming or vertical, so that the graph $\operatorname{Ext}\Gamma$ satisfies property (T2). Since the original graph is a tree, the extended graph is unique up to isotopy of the plane. Typical examples for $g = 1$ and $g = 2$ are given in Figure 2.

From the topological viewpoint all the components of the complement to the extended graph in the plane have the same structure. They are 2-cells bounded by exactly one vertical edge R and two finite chains of horizontal edges attached to the endpoints of R, all pointing away from the vertical edge and meeting at infinity. For each cell we denote by $h(R)$ the weight of the corresponding vertical edge and define the half-strip for $h = h(R)$ by

$$\Sigma(h) = \{\eta \in \mathbb{C} : \operatorname{Re}\eta > 0 \text{ and } 0 < \operatorname{Im}\eta < h\}.$$

We glue these $2\sharp\{\text{vertical edges}\}$ half-strips by translations along the horizontal edges and a rotation of angle π along the vertical edges as indicated by the graph $\operatorname{Ext}\Gamma$. This flat structure

https://doi.org/10.1112/S0010437X25007158 Published online by Cambridge University Press

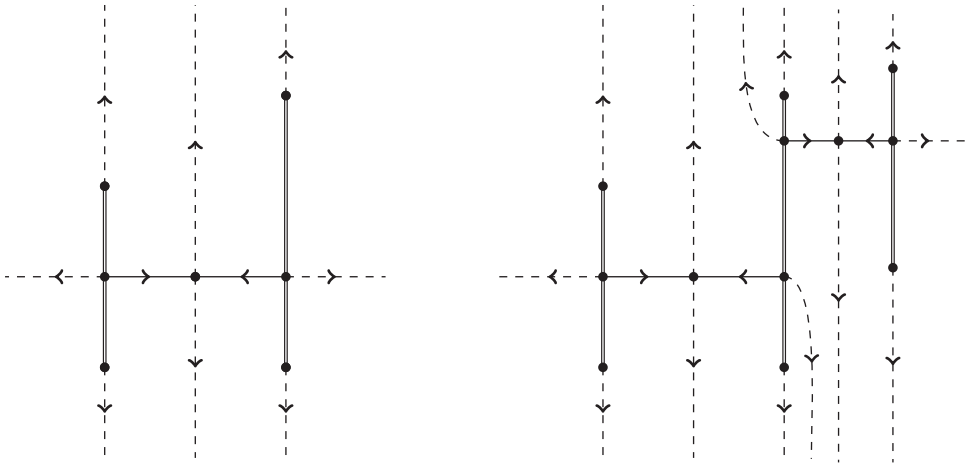


Figure 2. The extensions of the graphs of Figure 1.

on the Riemann sphere has $2g+2$ singularities of odd order and is well defined up to the action of the affine group. The Riemann surface M is defined to be the double cover ramified at these points. The distinguished quadratic differential on the Riemann sphere is the one whose flat structure has just been defined. □

Remark 4.

(1) The axiomatic description of the graphs Γ which appear as associated graphs of Riemann surfaces, including the five constraints (T1,T2,T3,W1,W2) and the realization theorem, were first established, for Riemann surfaces admitting an anticonformal involution (i.e. reflection), in [Bog12, Bog03]. The purely complex case is somewhat simpler as we should keep in mind that in the real case there is a mirror symmetry and additional topological invariants, splitting of homology, etc.

(2) An interesting enumerative problem related to the associated graphs arises: compute the number of (stable) combinatorial graphs Γ associated with the Riemann surfaces M of genus g. The same holds for real curves with a given genus, and the number of real ovals.

4.4 Period mapping in terms of graphs

In this section we explain how to compute the periods of the distinguished differential from a graph satisfying the conditions of Theorem 4.3.

4.4.1 *Homology basis associated with a graph.* Given a graph $\Gamma = \Gamma(M)$, we associate a set of $2g+2$ cycles on the twice-punctured surface $M = M_\infty \setminus \infty_\pm$ which generate its integer homology group $H_1(M,\mathbb{Z}) = \mathbb{Z}^{2g+1}$. This set is unique if all the branchpoints are pendent (degree one) vertices of the graph, which is the generic case; see the example in Figure 3.

We denote the complex plane cut along the vertical part of the graph by $M^+ := \mathbb{C} \setminus \Gamma_{\mathbf{I}}$. The Riemann surface M is obtained by gluing two copies of M^+ along the cuts in a criss-cross manner: each bank of a cut in a copy of M^+ is glued to the opposite bank of the same cut in the other copy.

Suppose that we travel counterclockwise along the boundary of the plane cut along the whole graph Γ. We meet each branchpoint e exactly once, provided that each of these branchpoints are hanging vertices of the tree. All the branchpoints therefore become cyclically ordered e.g.

https://doi.org/10.1112/S0010437X25007158 Published online by Cambridge University Press

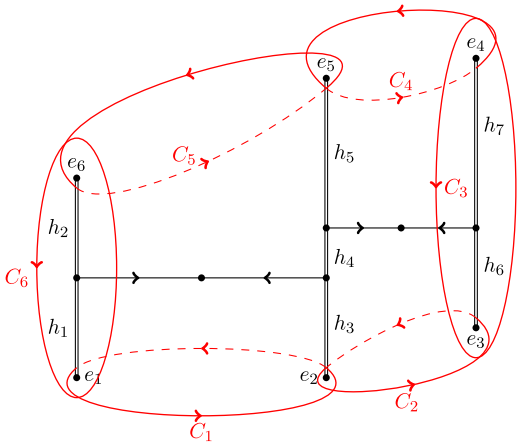


FIGURE 3 (colour online). Generators of the first homology group of the genus $g=2$ Riemann surface associated with the generic graph Γ.

$e_1, e_2, \dots, e_{2g+2}, e_{2g+3} = e_1$. If there are interior branchpoints, some points $e \in \mathsf{E}$ will be listed more than once, and we eliminate all duplicates in an arbitrary way. We again get a cyclic order of all the branchpoints, although it is not unique.

For $j = 1, \dots, 2g+2$, let c_j be any simple arc connecting point e_j to e_{j+1} that is disjoint from the graph Γ except for its ends. We draw this arc on M^+, and then $C_j := (\mathrm{Id} - J)c_j$ is a closed loop on the surface M. These $2g+2$ loops are represented in Figure 3. They are linearly dependent: both sums of the loops with even/odd indexes are equal to the same loop encircling the puncture ∞_+ clockwise. There are no other relations between them.

LEMMA 4.4. *The cycles $C_1, C_2, \dots, C_{2g+1}$ make up a basis of the lattice $H_1(M, \mathbb{Z})$.*

Proof. For every $j = 1, \dots, 2g+2$ consider the relative cycles D_j in the relative homology group $H_1(M_\infty, \{\infty_\pm\}, \mathbb{Z})$ given by $D_j := (\mathrm{Id} - J)d_j$, where d_j is any simple arc connecting the branchpoint e_j to ∞_+ that is disjoint from the graph except for its starting point. There is a pairing between the above two homology groups given by the intersection index. We compute that $D_s \circ C_j$ is equal to 1 if $s = j$ or $s = j+1$ and is equal to 0 for all other indexes. The determinant of the intersection matrix $\|D_s \circ C_j\|_{s,j=1}^{2g+1}$ is equal to 1. □

4.4.2 *Period mapping for the associated homology basis.* Given an admissible graph Γ, we can calculate the periods of the distinguished differential $d\eta$ along the basic cycles C_j introduced in § 4.4.1. This differential may be reconstructed from the width function as $d\eta = 2\partial W(z)$ on the top sheet M^+. On the other sheet it just has the opposite sign.

LEMMA 4.5. *The period of the distinguished differential $d\eta$ along the cycle C_j is*

$$\int_{C_j} d\eta = 2i \sum_{e_j < R < e_{j+1}} h(R), \tag{11}$$

where the summation is taken over all vertical edges R of Γ that appear when travelling counterclockwise from e_j to e_{j+1} along the bank of Γ.

Proof. Let $H(z)$ be the harmonic conjugate to the width function $W(z)$. It is a multi-valued function in the complement of the graph Γ: going around the graph (or equivalently, the infinity)

https://doi.org/10.1112/S0010437X25007158 Published online by Cambridge University Press

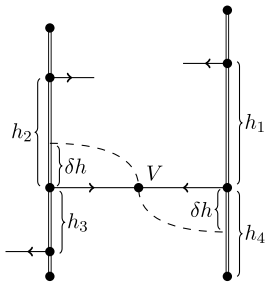


Figure 4. Vicinity of a generic saddle point V. The horizontal segment of the graph deformed by $h_s \to h_s - (-1)^s \delta h$ with positive δh is pictured as a dashed curve.

adds $\pm 2\pi$ to the initial value of $H(z)$. We have a chain of equalities:

$$\int_{C_j} d\eta = 2 \int_{c_j} d\eta = 2 \int_{c_j} d(W + iH) = 2i \int_{c_j} dH. \tag{12}$$

To obtain the last equality we use the fact that the width function W vanishes at all the branchpoints e, where the path c_j starts and ends. Continuing the last equality:

$$\int_{C_j} d\eta = 2i \sum_{e_j < R < e_{j+1}} \int_R dH = 2i \sum_{e_j < R < e_{j+1}} h(R). \tag{13}$$

Here we use the Cauchy–Riemann equations

$$dH|_R = \frac{\partial W}{\partial n} dl,$$

where n is normal to the edge R and l is a length parameter on the edge. Hence dH vanishes at the horizontal edges and is equal to the metric of the differential $|d\eta|$ on the vertical edges. □

Example 4.6. For the graph pictured in Figure 3, the period of $d\eta$ along the cycle C_1 is $2i(h_1 + h_3)$, the period along the cycle C_2 is $2i(h_3 + h_4 + h_6)$, and the period along the cycle $C_1 + C_3 + C_5$ is $2i(h_1 + h_3 + h_6 + h_7 + h_5 + h_4 + h_2) = 2\pi i$, according to the normalization property (W2).

4.5 Local isoperiodic deformations

We know from Theorem 3.1 that fixing the values of the periods of the distinguished differential locally defines a complex $(g+2)$-dimensional submanifold, such as $\tilde{\mathscr{A}}_g^n$, in the moduli space $\tilde{\mathcal{H}}_g$. Two degrees of freedom on this manifold account for the inessential affine motions of the branching divisor which do not change the complex structure. The remaining g complex degrees of freedom on the isoperiodic manifold may be explained in terms of the associated graphs. For simplicity we define the isoperiodic deformations for the generic graph, and the general case will follow from continuity.

In the generic case, the width function W has exactly g saddle points V, which are the double zeros of $(d\eta)^2$. The vicinity of each of these saddle points in the graph Γ has the appearance shown in Figure 4: the vertex V is the meeting point of exactly two horizontal edges which go straight from two vertical components of the graph. Each of the two nearest neighbour nodes of V is incident to exactly two vertical edges. We label the weights of these four vertical edges nearest to V cyclically as h_1, h_2, h_3 and h_4, as in Figure 4. The following two modifications of the weights in the neighbourhood of the vertex V obviously do not change any period:

$$W(V) \to W(V) + \delta W; \quad h_s \to h_s - (-1)^s \delta h, \quad s = 1, 2, 3, 4, \tag{14}$$

https://doi.org/10.1112/S0010437X25007158 Published online by Cambridge University Press

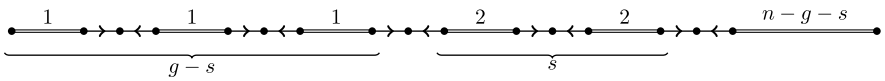


Figure 5. The linear graph $\Gamma(s,g,n)$ for $g=5$ and $s=2$.

with real increments δW, δh small enough for the modified graph to obey the admissibility conditions.

We will use deformations of this kind to bring the graph of a Riemann surface M corresponding to (PA) that admits a primitive solution of degree n to a standard form.

5. Isoperiodic deformations to graphs of standard forms

The original enumeration problem essentially belongs to algebraic geometry, but graph technology allows us to study it by efficient combinatorial methods. A similar approach is used in the classification of the connected components of the strata of abelian differentials [KZ03], in intersection theory on moduli spaces [Kon91, Kon92], and in some other investigations.

In this section we first introduce two standard forms of the graphs $\Gamma(M)$, and then present a combinatorial procedure for the isoperiodic deformation of a graph associated with a Pell–Abel equation with a primitive solution of degree n to a standard form graph.

These standard forms may be chosen in different ways. For the upper bound of the number of connected components $a(g,n)$, we use the *two-bush* standard form. For the lower bound in § 6.2 we use the *linear* standard form. For the sake of completeness we give an explicit isoperiodic transformation between the two standard forms.

5.1 Two standard forms of graphs

Let Γ be a graph associated with a Pell–Abel equation with a primitive solution of degree n. For convenience we rescale the weights of its vertical edges as follows:

$$\hbar(R) := nh(R)/\pi. \tag{15}$$

This rescaling allows us to work with integers instead of rational multiples of π. To distinguish between the normalizations, we continue to call the value $h(R)$ the weight of the (vertical) edge R, whereas we refer to $\hbar(R)$ as its *height*. Note that the total height of the vertical component of a graph is equal to n.

Definition 5.1. The linear graph $\Gamma(s,g,n)$ with integer parameters $g\geqslant 1$, $n\geqslant g+1$ and $s=0,1,\dots,m^*:=\min(g-1,n-g-1)$ is defined as follows. It has $g+1$ vertical segments connected at their endpoints by g horizontal components so that the whole graph is embedded in a line, as represented in Figure 5. The first $(g-s)$ vertical edges are of height $\hbar=1$ and these are followed by s vertical edges of height $\hbar=2$; finally the height of the last edge is $\hbar=n-g-s$. The value of the width function at its g saddle points is not specified as it is inessential.

Remark 5. The number s of vertical edges of height $\hbar=2$ in the standard linear form cannot be too large when the degree n is smaller than $2g$. If it was too large, the last vertical edge would have zero or negative height. This is the reason why s is less than or equal to $m^*:=\min(g-1,n-g-1)$.

Remark 6. The linear graphs correspond to Riemann surfaces M with only real branchpoints. The solutions $P(x)$ of the corresponding Pell–Abel equations are known as multiband Chebyshev

https://doi.org/10.1112/S0010437X25007158 Published online by Cambridge University Press

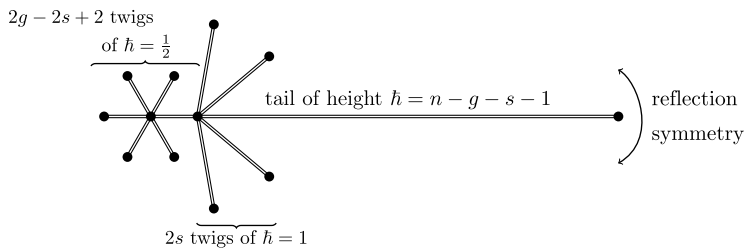


FIGURE 6. The two-bush graph $\Gamma^*(s,g,n)$ for $g=4$ and $s=2$.

polynomials; see [Bog99, Bog03]. In this case, the heights $\hbar$ of the vertical segments correspond to the oscillation numbers of the Chebyshev polynomial $P(x)$ on the bands. In general, they can take arbitrary positive integer values which sum up to $\deg P=n$.

Given the same set of parameters (s,g,n) as we had for the standard linear form $\Gamma(s,g,n)$, we introduce the *two-bush* standard form $\Gamma^*(s,g,n)$ built as follows.

DEFINITION 5.2. The small bush is a collection of $2(g-s)+2$ vertical edges, that we call twigs, of equal height $\hbar=1/2$, all growing from the same root. The large bush is a similar starlike graph of $2s$ vertical edges of height $\hbar=1$. The two-bush graph $\Gamma^*(s,g,n)$ is obtained by gluing the root of the large bush and a vertical edge of height $\hbar=n-g-s-1$, called the tail, to a hanging vertex of the small bush, in such a way that the whole embedded graph admits reflection symmetry. Such a graph is pictured in Figure 6.

Note that the tail disappears when $s=n-g-1$. In this case, the root of the larger bush becomes a branchpoint.

We will prove in § 5.3 that these two standard forms are related to each other in the following way.

LEMMA 5.3. *The two-bush graph $\Gamma^*(s,g,n)$ and the linear graph $\Gamma(s,g,n)$ are joined by an isoperiodic deformation.*

The two-bush graphs $\Gamma^*(s,g,n)$ and $\Gamma^*(s-1,g,n)$ with $s>0$ and $s+g+n$ odd are joined by an isoperiodic deformation.

The main result of this section is the following.

THEOREM 5.4. *Any graph Γ corresponding to a Pell–Abel equation $P^2(x)-D(x)Q^2(x)=1$ with $\deg D=2g+2>2$ and admitting a primitive solution of degree $n>g$ can be isoperiodically transformed into a two-bush graph $\Gamma^*(s,g,n)$ for some $s=0,1,\dots,m^*$, where m^* is the minimum of $\{g-1,n-g-1\}$.*

COROLLARY 6. *The number of connected components $a(g,n)$ of $\mathscr{A}_g^n$ for $n>g$ and $g>0$ is at most $[m/2]+1$ if $n+g$ is odd and at most $[(m+1)/2]$ if $n+g$ is even, where*

$$m=\min(g,n-g-1).$$

Proof. According to Lemma 5.3, the two-bush graphs $\Gamma^*(s,g,n)$ and $\Gamma^*(s-1,g,n)$ can be joined by an isoperiodic deformation if $s>0$ and $s+g+n$ is odd. Now it suffices to count the parameters to see that the number of nonequivalent two-bush graphs is at most $[(m+1)/2]$ when $n+g$ is even and $[m/2]+1$ when $n+g$ is odd. □

https://doi.org/10.1112/S0010437X25007158 Published online by Cambridge University Press

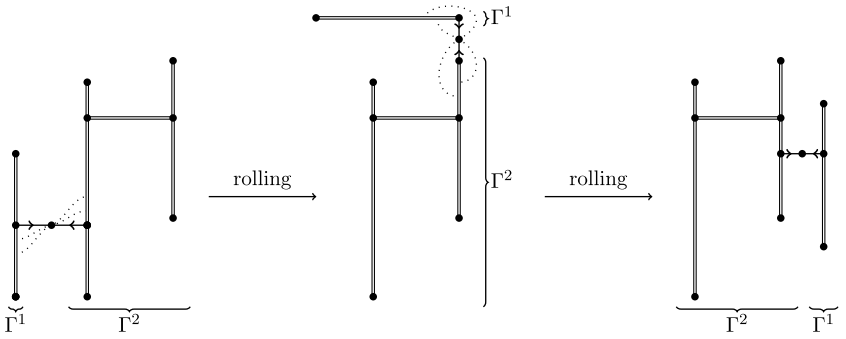


FIGURE 7. Rolling the vertical component $\Gamma_{\mathbf{I}}^1$ around the core component $\Gamma_{\mathbf{I}}$. The dotted lines show the intermediate positions of the chord.

In order to prove Lemma 5.3 and Theorem 5.4 we present some preparatory material on isoperiodic deformations.

5.2 Useful isoperiodic deformations

In this preparatory section, we describe some useful isoperiodic deformations of a graph associated with hyperelliptic Riemann surfaces M_∞ with a pair of marked points $\infty_\pm$ in involution.

5.2.1 *Rolling.* Suppose that the graph Γ has exactly two disjoint vertical components $\Gamma_{\mathbf{I}}^1$ and $\Gamma_{\mathbf{I}}^2$. The latter are connected by the only horizontal component containing exactly two edges meeting at the saddle point of the width function, as shown on the left of Figure 7. We call such a simple horizontal component a *cord*.

The following deformation of Γ, called *rolling* and pictured in Figure 7, is isoperiodic. The cord is fixed while the two vertical components rotate as rigid bodies in the same direction so that the meeting points of the cord with the two vertical components move along the boundaries of $\Gamma_{\mathbf{I}}^1$ and $\Gamma_{\mathbf{I}}^2$ with equal speed. Alternatively, we keep one of the vertical components, say $\Gamma_{\mathbf{I}}^2$, static, and we now call this the *core* component. The cord goes around the core and drags the other vertical component $\Gamma_{\mathbf{I}}^1$ which at the same time rotates with respect to the cord in the opposite direction, so that the equality of velocities of the contact points again holds. Essentially this deformation is the same as that in § 4.5, except that the parameter δh of the deformation is no longer small.

Remark 7. The rolling of a pendent vertical component of the graph Γ around the rest of the graph may be defined in a more general case. For simplicity, we do not use any deformations in this paper which lead to the collision of different horizontal components of the graph. A collision of this type leads to a deeper change in the combinatorial structure of the graph Γ; see e.g. [Bog12, Chapter 4] and [Bog23] for the analytical aspects of such a collision.

5.2.2 *Attaching and detaching.* Given a graph Γ and the rolling procedure, the cord may be contracted when it reaches some point V at the boundary of the core graph $\Gamma_{\mathbf{I}}^2$ during rolling. This procedure is called the *attaching* of $\Gamma_{\mathbf{I}}^1$ at the point V on the core vertical graph. Note that if the cord connects two branchpoints, as it does in the middle of Figure 7, the procedure leads to a nodal curve M and is prohibited. The inverse procedure of inserting a cord at a vertex V of a vertical subgraph will be referred to as a *detaching*.

https://doi.org/10.1112/S0010437X25007158 Published online by Cambridge University Press

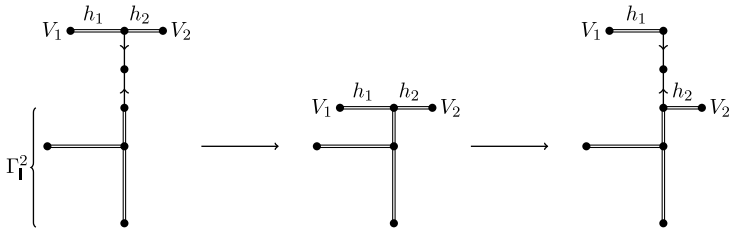


FIGURE 8. Pumping mass from a pendent vertical segment $[V_1, V_2] = \Gamma_{\mathbf{I}}^1$ to the core graph $\Gamma_{\mathbf{I}}^2$.

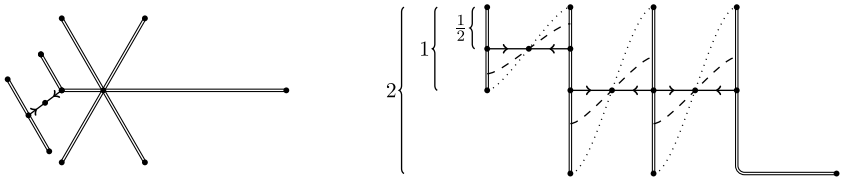


FIGURE 9. The two-bush form $\Gamma^*(s, g, n)$ with $s = 2$ and $g = 3$ just after detaching the first pair of small twigs, and its deformation into the standard line form $\Gamma(s, g, n)$. The numbers designate the heights of the edges.

5.2.3 *Pumping.* Given a graph Γ with a pendent vertical segment $[V_1, V_2] = \Gamma_{\mathbf{I}}^1$ and a core graph $\Gamma_{\mathbf{I}}^2$, we can roll $\Gamma_{\mathbf{I}}^1$ until the cord passes through a branchpoint of $\Gamma_{\mathbf{I}}^2$, as pictured on the left of Figure 8. We can transfer a positive weight from $\Gamma_{\mathbf{I}}^1$ to the core component by the following *pumping* construction. We first contract the cord as shown in the middle of Figure 8, and then insert it again in another way as shown on the right of Figure 8.

Note that pumping the mass is impossible if the cord simultaneously passes through two branchpoints, one on the pendent vertical segment and the other on the core graph, as can be seen in the middle of Figure 7. As observed before, contracting the cord in such a case brings us to a nodal curve.

5.3 Proof of Lemma 5.3

Starting with the two-bush graph, we detach $(g - s)$ pairs of consecutive little twigs with $\hbar = 1/2$ from their root. The graph, after detaching the first pair, is shown on the left of Figure 9. We do the same for the pairs of consecutive big twigs with $\hbar = 1$, and obtain the graph on the right of Figure 9. Finally, it suffices to 'rotate' each horizontal segment counterclockwise to obtain the linear graph. The intermediate positions of the horizontal components are indicated by dotted/dashed lines on the right-hand side of the same Figure 9.

For the deformation from the two-bush graph $\Gamma^*(s, g, n)$ to $\Gamma^*(s - 1, g, n)$, we detach a bunch of $(g - s)$ pairs of neighbouring twigs from the small bush, roll the bunch and attach it to the midpoint of the neighbouring twig of the large bush, provided $s > 0$, as shown on the left of Figure 10. We obtain $s - 1$ twigs of unit height on the right of the new small bush and $s + 1$ twigs of $\hbar = 1$ to the right counted from the root of the large bush. Now we detach a couple of neighbouring unit height twigs from the larger part of the large bush, roll the $\hbar = 2$ pendent vertical segment and attach it to the endpoint of the tail. Since the height of the tail is even we get the graph on the right of Figure 10. A unit height edge incident to the endpoint of the tail may be detached, rolled toward the small bush, and attached to its root. Thus we obtain the standard graph $\Gamma^*(s - 1, g, n)$.

https://doi.org/10.1112/S0010437X25007158 Published online by Cambridge University Press

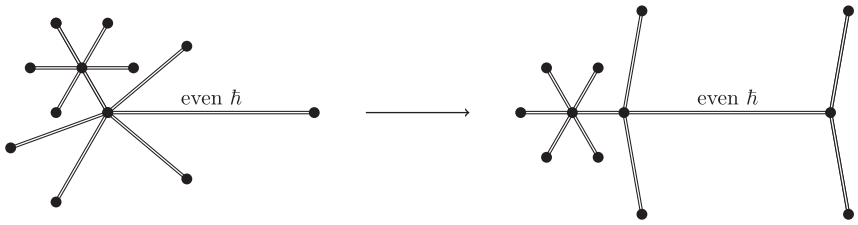


Figure 10. An isoperiodic deformation between the bush graphs $\Gamma^*(s,g,n)$ and $\Gamma^*(s-1,g,n)$ when $s+g+n$ is odd.

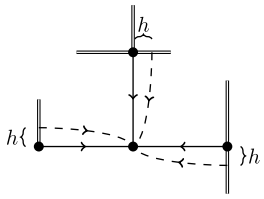


Figure 11. Clockwise rotation of a component of $\Gamma_{_}$. The new position of the horizontal component is shown with the dashed curve.

5.4 Proof of Theorem 5.4

Let $\Gamma(M)$ be a weighted graph associated with a Riemann surface M of genus $g>0$ corresponding to (PA) with a primitive solution of degree $n \geqslant g+1$. We prove that $\Gamma(M)$ may be isoperiodically deformed to the two-bush graph $\Gamma^*(s,g,n)$ for some $s=0,1,\dots,m^*$, where $m^* := \min(g-1, n-g-1)$.

The proof is split into several consecutive steps:

(1) collapsing the horizontal component of the graph to obtain a purely vertical graph;
(2) detaching the vertical segment of minimal possible length $\hbar=1$; and
(3) bringing the core graph to the standard form by induction on the genus g.

Stage 1: *Obtaining a purely vertical graph.* Let $\Gamma(M)$ be any graph satisfying the hypothesis of Theorem 5.4. The elimination of its horizontal component may be achieved by linearly decreasing to zero the values of the width function $W(V)$ at all vertices V of the horizontal subgraph. The only drawback of this deformation is that some branchpoints may collide in the final instant of the deformation. To prevent this, we may preliminarily 'rotate' every horizontal component of the graph by shifting all its points of intersection with the vertical subgraph by the same small value δh in the same direction to avoid passing through the branchpoints. An example of the rotation is shown in Figure 11. After the contraction of its horizontal component, the graph is composed only of vertical edges.

Stage 2: *Creating a pendent segment of height* $\hbar=1$. Let us first show that there exist two hanging edges that are neighbouring with respect to the cyclic order around some vertex V of the graph. Indeed, take any vertex L of the graph Γ. Choose any vertex V_1 of Γ at the maximal path length from L (i.e. with the number of edges in the path joining them being maximal). This is necessarily a hanging vertex of Γ, and the previous vertex V in the path $[L,V_1]$ on the graph is at distance one less from L. The degree $d(V)=d_{\mathbf{I}}(V)>1$, since $g>0$, and moreover $d(V)\neq 2$ because of property (T3) of admissible graphs. Hence the node V is joined to yet another vertex

https://doi.org/10.1112/S0010437X25007158 Published online by Cambridge University Press

V_2 at the same distance from L as V_1. This vertex V_2 is also hanging, so the edges joining V to V_1 and V_2 are the desired ones.

We are going to create a pendent vertical segment of minimal height $\hbar = 1$ using the two transformations of *rolling* and *pumping*. Detach from the rest of the graph the vertical segment $[V_1, V_2] := \Gamma^1_{\mathbf{I}}$ obtained above. Then roll it around the core graph $\Gamma^2_{\mathbf{I}}$ and pump its mass whenever possible. Since the height of the segment is always an integer it cannot diminish ad infinitum. Hence it stabilizes at some integer $l \geqslant 1$. If $l > 1$, then all $\hbar$-distances between neighbouring branchpoints on the boundary of the core graph are divisible by l, and hence all the periods of $d\eta_M$ lie in the coarse lattice corresponding to the integer n/l. This would mean that the solution of degree n of Equation (PA) is not primitive.

This pendent vertical segment of height $\hbar = 1$ is called the *catalyst*. We can roll it to any convenient place in the rest of the graph where it does not interfere with further manipulations. In particular, for $g = 1$ we can attach it to the core graph to obtain the two-bush graph $\Gamma^*(0, 1, n)$, proving Theorem 5.4 in that case.

Stage 3: *Induction step for* $g \geqslant 2$. Let us consider the core graph $\Gamma^2_{\mathbf{I}}$ (obtained after detaching the catalyst) as a separate graph equipped with the present heights $\hbar$ of its vertical edges. Since $\Gamma^2_{\mathbf{I}}$ satisfies the conditions of Theorem 4.3, it corresponds to a Pell–Abel equation admitting a degree $n-1$ solution on a genus $g-1$ Riemann surface (explicitly described in the second part of the proof of Theorem 4.3). Once the solution is primitive, we bring the graph to the two-bush form $\Gamma^*(s, g-1, n-1)$ by the induction hypothesis. Then we roll the catalyst towards the smaller bush and attach it at its root. Thus we obtain $\Gamma^*(s, g, n)$ with parameter s in the admissible range of values.

Suppose now that the Pell–Abel equation corresponding to the core graph $\Gamma^2_{\mathbf{I}}$ admits a primitive solution of smaller degree $n' = (n-1)/l$ for some integer $l \geqslant 2$. By the induction hypothesis, the graph $\Gamma^2_{\mathbf{I}}$ may be isoperiodically transformed into a two-bush graph $\Gamma^*(s, g-1, n')$ which however uses another scale for the weights of the edges. To return to our initial units we should multiply all the heights of this graph by the integer factor $l = (n-1)/n'$.

Recall that the catalyst of unit height is joined to the rescaled two-bush core graph by a cord. We attach the catalyst to a hanging twig of the smaller bush (which exists in the worst case $s = g-1$) at a distance $\hbar = 1 \geqslant l/2$ from the endpoint. Then we detach the $\hbar = 2$ vertical segment (composed of the catalyst and part of the small bush twig) from the graph. The procedure is allowed even in the worst case $l = 2$. In that case the catalyst is attached to the root of the small bush, which is not a branchpoint.

We claim that the remaining core graph $\Gamma^{2'}_{\mathbf{I}}$ corresponds to (PA) admitting a primitive solution of degree $n-2$. Indeed, the $\hbar$ distances between the branchpoints along the boundary of $\Gamma^{2'}_{\mathbf{I}}$ are all integers and include the coprime numbers l and $l-1$ (on the small bush). Now the induction step may be applied again and we replace the core graph $\Gamma^{2'}_{\mathbf{I}}$ by the two-bush form $\Gamma^*(s, g-1, n-2)$. The pendent segment of height $\hbar = 2$ may be attached by its midpoint to the obtained two-bush form either:

(1) at the root of the large bush, as pictured on the left of Figure 12; or

(2) at the tip of the large bush twig (this happens only when $s > 0$), as shown in the upper left picture of Figure 13.

Case (1). We detach a bunch of $(g-s-1)$ pairs of twigs from the small bush, roll them and attach them to the midpoint of the nearest twig of the large bush, as illustrated on the right of Figure 12 where the dashed curves show the final positions of the horizontal components. Thus

https://doi.org/10.1112/S0010437X25007158 Published online by Cambridge University Press

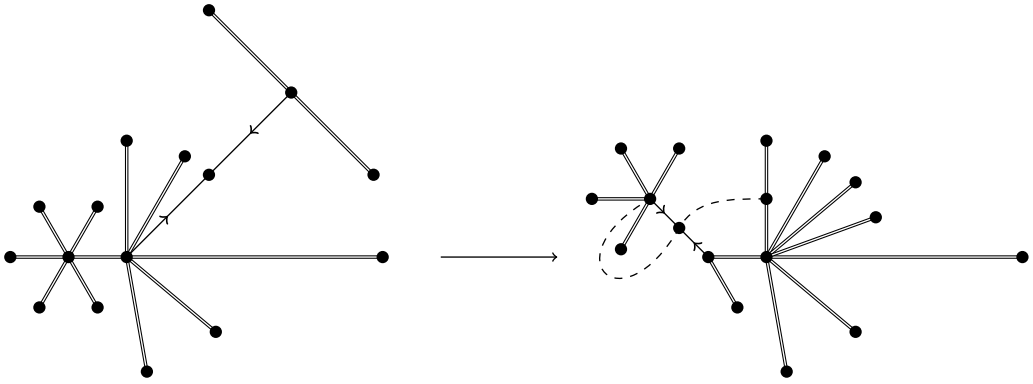


Figure 12. The induction step in case (1) for $g=5$ and $s=2$.

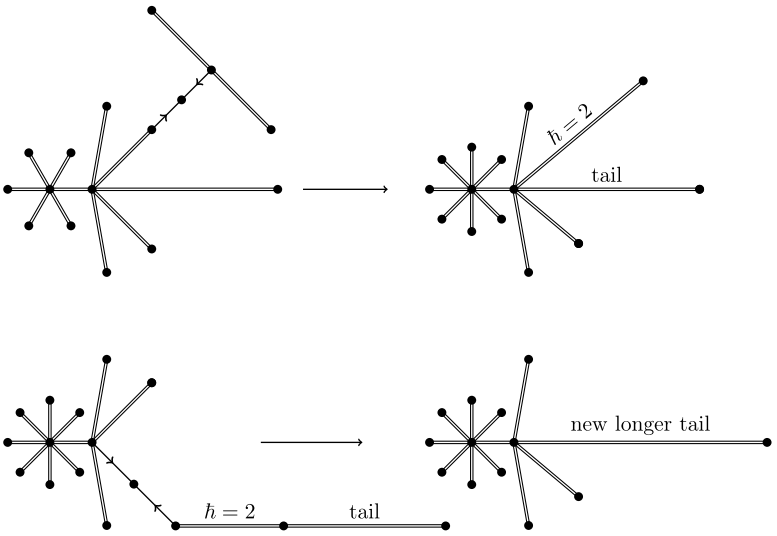


Figure 13. The induction step in case (2) for $g=5$ and $s=2$.

we obtain the graph $\Gamma^*(s+1,g,n)$. Note that $s+1$ is an admissible value of parameter for given g and n when $s\leqslant\min(g-2,n-g-2)$.

Case (2). Starting from the top left picture of Figure 13, we first attach the pendent segment. This creates a T-shape whose branches are of height 1. We detach one of the unit height twigs of the T-shape, roll it around the core graph and attach it to the root of the small bush as shown in the top right picture of Figure 13. Next, we detach the union of the tail (which may be of height 0) of the two-bush graph and the neighbouring $\hbar=2$ edge. We roll it along the neighbouring twig of height $\hbar=1$, as pictured at the bottom left of Figure 13. Finally, we attach it to the core graph at the root of the large bush, as pictured at the bottom right of Figure 13. The root of the larger bush is now a branchpoint, so one twig of this bush may be detached and replanted on the smaller bush as we have just done. We obtain the two-bush graph $\Gamma^*(s-1,g,n)$. This completes the proof of Theorem 5.4.

Remark 8. A proof without recursion is available too, but it is a bit longer and the deformations are more involved.

https://doi.org/10.1112/S0010437X25007158 Published online by Cambridge University Press

6. Isoperiodic invariants

In this section, we show that the genus g hyperelliptic Riemann surfaces associated with Pell–Abel equations admitting a primitive solution of degree n that correspond to nonequivalent linear graphs $\Gamma(s,g,n)$ as described in § 5.1 live in different components of $\mathscr{A}_g^n$. To this end, we introduce two global invariants of the isoperiodic transformation and compute them for all graphs $\Gamma(s,g,n)$.

The first invariant is based on the partition of the degree of the polynomial $D(x)$ of the Pell–Abel equation (PA) into two summands. For this reason we call it the *degree partition invariant*. Its elementary construction is given in § 6.1. We describe a way to compute it using graphs, and show that each admissible partition is realized by a unique linear graph $\Gamma(s,g,n)$. This completes the proof of Theorem 1.2 and the reader could stop there.

The other invariant described in § 6.2 possesses a much richer geometric content: it is related to braids, which describe the motions of unordered branching sets E in the plane without collisions of any individual branchpoints. Hence this invariant is referred to as the *braid invariant*. The construction of this invariant is far less elementary, but nonetheless it numerically coincides with the degree partition invariant. However, it gives a deeper immersion into the geometry of the problem and will, no doubt, be used for further research on the topic.

6.1 Degree partition invariant

The value of a solution P of (PA) at a zero $e \in \mathsf{E}$ of the polynomial D may be either $+1$ or -1. Therefore, the set E of zeros of D is split into two subsets $\mathsf{E}^{\pm}$. Since we cannot globally distinguish between solutions P and $-P$, we consider the cardinalities of those sets as an unordered partition of $|\mathsf{E}| = \deg D := 2g+2$. In particular, we may assume that

$$|\mathsf{E}^-| \leqslant g+1 \leqslant |\mathsf{E}^+|.$$

The *degree partition invariant* of $D \in \mathscr{A}_g^n$ is the unordered pair $(|\mathsf{E}^-|, |\mathsf{E}^+|)$ computed for the primitive solution $\pm P(x)$.

This invariant is easily computable from the graph Γ of the associated curve. The $\hbar$-distance between any two branchpoints of the curve along the boundary of the graph should be an integer. It may be either even or odd, depending on whether those branchpoints lie in the same set $\mathsf{E}^{\pm}$ or in different sets. To compute the value of the solution P at any branchpoint e_s we use (5). The integral of the distinguished differential between e_1 and e_s has already been computed in § 4.4.2 in terms of the weights h: it is the sum of all the vertical weights of the edges on a path between e_1 and e_s along the boundary of Γ. Now, by substituting the heights $\hbar$ of the edges in place of their weights h, we get the justification of the above rule.

Lemma 6.1. *The degree partition invariant* $(|\mathsf{E}^-|, |\mathsf{E}^+|)$ *of* $D \in \mathscr{A}_g^n$ *having a primitive solution* P *of degree* n *satisfies:*

(1) $|\mathsf{E}^{\pm}| > 0$,
(2) $|\mathsf{E}^{\pm}| \leqslant n$, *and*
(3) *the parity of* $|\mathsf{E}^{\pm}|$ *is equal to the parity of* n.

Proof.
(1) Note that in the graph description, $|\mathsf{E}^-| = 0$ exactly when all the boundary $\hbar$-distances between the branchpoints are even. Dividing all the heights of the graph by 2, we get a solution P of degree twice less.

https://doi.org/10.1112/S0010437X25007158 Published online by Cambridge University Press

(2) A nontrivial polynomial has at most a number of roots equal to its degree.
(3) The set E of roots of D is the set of $x \in \mathbb{C}$ where P takes the value ± 1 with odd multiplicity. □

Finally, we compute the degree partition invariant of a linear graph.

Example 6.2. The degree partition invariant of the linear graph $\Gamma(s, g, n)$ has the following smaller element:

$$|\mathsf{E}^-| = g - s + \alpha, \tag{16}$$

where $\alpha = (s + g + n) \mod 2 \in \{0, 1\}$. We note that all linear graphs $\Gamma(s, g, n)$ correspond to different partitions (and therefore belong to different components of $\mathscr{A}_g^n$) outside the cases explicitly described in Lemma 5.3.

Remark 9. One can check, by direct calculation, that the number of the values taken by this invariant is exactly the number $a(g, n)$ of components in Theorem 1.2. This completes its proof.

To conclude this subsection, we compute the partition invariant of a Riemann surface defined over $\mathbb{Q}$.

Example 6.3. In [Pla14, p. 30] it is shown that the Pell–Abel equation (PA) with the polynomial

$$D(x) = x^6 + 6x^4 + 33x^2 + 24$$

has the primitive solution

$$P(x) = \tfrac{1}{24}x^9 + \tfrac{3}{8}x^7 + \tfrac{9}{4}x^5 + 6x^3 + 9x \quad \text{and} \quad Q(x) = \tfrac{1}{24}x^6 + \tfrac{1}{4}x^4 + x^2 + 1.$$

Now it is easy to check numerically that the vector of the values of P at the roots of D contains 3 times $+1$ and 3 times -1. Hence D belongs to the component of degree partition invariant $(3, 3)$.

6.2 Braid invariant

We know what the invariance of periods means for small deformations of the branching set E (see, for example, the discussion at the end of § 3). For large deformations, we need some way to identify the integration cycles on remote surfaces $M(\mathsf{E})$. This is done via the parallel transport of cycles using the Gauss–Manin connection (see [Vas95, § I.1] or [Bog12, Chapter 5]).

Suppose that we move the branchpoints and simultaneously distort a cycle C so that the branchpoints never cross its projection to the x-plane. In this way we transport the cycle along some path τ in the space $\tilde{\mathcal{H}}_g$ of hyperelliptic Riemann surfaces with a pair of marked points at infinity (identified with the space of complex monic square-free polynomials $D(x)$ of degree $2g + 2$). The resulting cycle belongs to the Riemann surface corresponding to the end of the path, and we denote it as $C \cdot \tau$, whereas C itself belongs to the Riemann surface at the beginning of the path. This action of paths on the homology spaces of the Riemann surfaces in $\tilde{\mathcal{H}}_g$ is associative: $C \cdot (\tau \cdot \sigma) = (C \cdot \tau) \cdot \sigma$ provided all products are correctly defined (e.g. the end of τ is the beginning of σ, etc.).

6.2.1 *Braids and isoperiodic deformations.* Fix an affine hyperelliptic Riemann surface M_1 whose branchpoints $e_1 < e_2 < \cdots < e_{2g+2}$ are real. We introduce the standard homology basis $C_1, C_2, \ldots, C_{2g+1}$ of $H_1(M_1, \mathbb{Z})$, where the projection of C_i to the x-plane encircles e_i and e_{i+1}, as pictured in the left-hand panel of Figure 14. Any Riemann surface M_2 of the same genus g

https://doi.org/10.1112/S0010437X25007158 Published online by Cambridge University Press

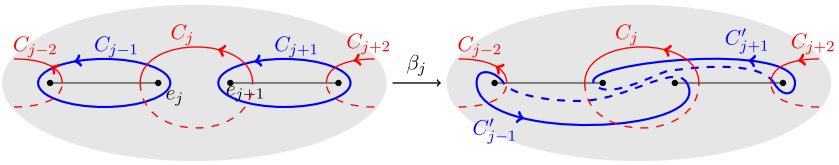


FIGURE 14 (colour online). The standard homology basis for a purely real Riemann surface M on the left, and the transport of basic cycles under the Dehn half-twist on the right. The slits pairwise joining the branchpoints are the pictured segments.

with purely real branchpoints may be connected to M_1 by a path σ in the space $\tilde{\mathcal{H}}_g$ such that all the branchpoints move along the real axis during the deformation. The transport of the standard homology basis for the starting surface along σ is the standard basis for the ending surface. Note that σ usually does not conserve any period.

Suppose that an isoperiodic path τ in $\tilde{\mathcal{H}}_g$ connects M_1 to M_2, both with real branchpoints (intermediate Riemann surfaces of the path may have general branchpoints). Let $d\eta_j$ be the distinguished differential on M_j defined in § 2. For every cycle $C_j \in H_1(M_1, \mathbb{Z})$ the following equalities hold:

$$\int_{C_j} d\eta_1 = \int_{C_j \cdot \tau} d\eta_2 = \int_{C_j \cdot (\tau \cdot \sigma^{-1}) \cdot \sigma} d\eta_2 = \sum_{r=1}^{2g+1} B_{jr}(\tau \cdot \sigma^{-1}) \int_{C_r \cdot \sigma} d\eta_2. \tag{17}$$

Here, the path $\beta := \tau \cdot \sigma^{-1}$ is a loop in the space $\tilde{\mathcal{H}}_g$ with the base point M_1, and it is represented by a braid $\beta \in \mathrm{Br}_{2g+2}$ on $2g+2$ strands. The transport of cycles along the loops by the Gauss–Manin connection has nontrivial holonomy. Given a standard basis of $H_1(M_1, \mathbb{Z})$, the holonomy is given by the matrix $B(\beta) = \|B_{jr}\| \in \mathrm{SL}_{2g+1}(\mathbb{Z})$. It is easy to calculate this matrix for an elementary braid β_r corresponding to the Dehn half-twist [Bir75] interchanging the branchpoints e_r and e_{r+1} counterclockwise for $r = 1, 2, \ldots, 2g+1$ (see right-hand panel of Figure 14):

$$(C_1, C_2, \ldots, C_{2g+1}) \cdot \beta_r = (\ldots, C_{r-1} - C_r, C_r, C_{r+1} + C_r, \ldots). \tag{18}$$

The braid β_r changes only the two homology cycles C_{r-1} and C_{r+1}. This matrix representation of the braids group is known as the *reduced Burau representation* $\mathcal{B}_t$ (see [GG06, § 2]) evaluated at the parameter $t = -1$.

It follows from this discussion that the naturally ordered periods of two linear graphs connected by an isoperiodic deformation lie in the same orbit of the representation $B(\beta)$. However the braid group is infinite and the fact that two vectors belong to the same orbit is difficult to check. For this reason we consider a coarser invariant when the periods are discrete. We consider the binary arrays of length $2g+1$. Obviously, the Burau representation modulo 2 acts on such binary strings too, but any orbit is now finite. We are interested in the orbits of the binary arrays of the form

$$(\hbar_1 \hbar_2 \hbar_3 \ldots \hbar_{2g+1}) \mod 2 \quad \text{with } \hbar_r := \frac{n}{2\pi i} \int_{C_r} d\eta_M \in \mathbb{Z}, \tag{19}$$

being the rescaled periods of the distinguished differential, $r = 1, 2, \ldots, 2g+1$. Note that, for totally real curves M, all entries $\hbar_r$ with even indexes r are zeros and the total sum of $\hbar_r$ is n.

Our immediate goal is to learn how to distinguish the orbits of the Burau representation reduced mod 2 on the binary arrays.

6.2.2 *Orbits of the Burau action reduced modulo* 2. Consider the following generating set in $\mathbb{Z}_2^{2g+1}$ that can be thought of as elements in $H^1(X, \mathbb{Z}_2)$ written in the basis dual to the C_i

https://doi.org/10.1112/S0010437X25007158 Published online by Cambridge University Press

introduced at the beginning of § 6.2.1:

$$\begin{aligned} v_1 &= (1000000\ldots0000);\\ v_2 &= (1100000\ldots0000);\\ v_3 &= (0110000\ldots0000);\\ v_4 &= (0011000\ldots0000);\\ &\vdots\\ v_{2g+1} &= (000000\ldots0011);\\ v_{2g+2} &= (000000\ldots0001). \end{aligned} \tag{20}$$

The only nontrivial linear relation between these vectors is $\sum_{r=1}^{2g+2} v_r = 0$. An elementary braid β_r acting on this set via the reduced Burau representation modulo 2 behaves like a transposition of two neighbouring elements:

$$v_r B(\beta_r) = v_{r+1},\ v_{r+1}B(\beta_r) = v_r \quad \text{and} \quad v_j B(\beta_r) = v_j \quad \text{when } j \neq r, r+1.$$

Therefore the braid group acts as a permutation group on the elements v_i of the generating set. It follows that the length Q of the shortest decomposition (there are exactly two of them) of the elements $v \in \mathbb{Z}_2^{2g+1}$ into the generators v_r with $r = 1, \ldots, 2g+2$ is the only invariant of our braid action on binary strings. This number Q is the *braid invariant* of the array. Note that it takes a value in $\{1, 2, \ldots, g+1\}$ and distinguishes the orbits of action of the Burau representation of braids on binary arrays.

Remark 10. Looking more carefully at its action on the set of generators v_i, it can be shown that the group generated by the reduced Burau matrices reduced mod 2 in $\mathrm{SL}_{2g+1}(\mathbb{Z}_2)$ is isomorphic to the symmetric group on $2g+2$ elements.

6.2.3 *The braid invariant of standard forms.* Let us calculate the value of the braid invariant Q for the hyperelliptic curves with associated linear graphs $\Gamma(s, g, n)$ for $s = 0, \ldots, m^*$ where $m^* := \min(g-1, n-g-1)$ (recall Remark 5 for the justification of the definition of m^*). The binary array corresponding to the latter graph is W_{g-s}, where

$$W_s = (1010101\cdots0101000\cdots000b) \quad \text{where } b(s) := (n+s) \mod 2, \tag{21}$$

with exactly s entries 1 in the first $2g$ places. These vectors satisfy the recurrence relation given by $W_s = v_{2s-1} + v_{2s-2} + W_{s-2}$ which, together with the initial conditions $W_1 = v_1 + bv_{2g+2}$ and $W_2 = v_2 + v_3 + bv_{2g+2}$, gives us the value of the braid invariant of the vectors W_s. Indeed, let $\alpha := (s+n+g) \mod 2$ with values 0 and 1, then the invariant is

$$Q(W_{g-s}) = g - s + \alpha \leqslant g+1. \tag{22}$$

Hence, the values of Q coincide for the equivalent graphs $\Gamma(s, g, n)$ and $\Gamma(s-1, g, n)$ when $g+n+s$ is odd, and are different for all the other graphs.

We conclude by comparing the braid invariant with the degree partition invariant.

Proposition 6.4. *The braid invariant Q of the vector of $\hbar$-heights of the linear graph coincides with the smaller number $|E^-|$ of the degree partition invariant $(|E^-|, |E^+|)$.*

Proof. It suffices to compare (22) with (16). □

https://doi.org/10.1112/S0010437X25007158 Published online by Cambridge University Press

7. k-differentials on hyperelliptic Riemann surfaces

In this last section, we prove Corollary 4. We begin by recalling some known facts on k-differentials and their moduli spaces. More information can be found in [BCG+19].

Given integers $g \geqslant 0$ and $k \geqslant 1$, a k-differential ξ on a genus g Riemann surface M is a non-zero section of the kth tensorial product of the canonical bundle K_M. A k-differential is said to be primitive if it is not the power of a k'-differential with $k' < k$.

Given a partition $\mu = (m_1, \ldots, m_n)$ of $k(2g-2)$, we consider the moduli spaces of k-differentials whose orders of zeros are equal to $m_1, \ldots, m_n$. This moduli space is called a *stratum* of k-differentials of type μ and is denoted $\Omega^k\mathcal{M}_g(\mu)$. The sublocus parametrizing the primitive k-differentials of type μ is denoted by $\Omega^k\mathcal{M}_g(\mu)^{\mathrm{prim}}$.

We now compute the number of connected components of the restriction of the strata of k-differentials with a unique zero to the hyperelliptic locus.

Proposition 7.1. *For $g \geqslant 2$, the number of connected components of the restriction of the strata $\Omega^k\mathcal{M}_g(k(2g-2))^{\mathrm{prim}}$ to the hyperelliptic locus is*

- $[(g-1)/2]$ *if* $k = 2$;
- 1 *if* $k = 3$ *and either* $g = 2$ *or* $g = 3$;
- $g/2$ *if* $k \geqslant 4$ *and* $g \geqslant 2$ *are even;*
- $g/2 + 1$ *if either* $g = 2$ *and* $k \geqslant 5$ *is odd, or* $k \geqslant 3$ *is odd and* $g \geqslant 4$ *is even; and*
- $(g+1)/2$ *if* $g \geqslant 3$ *is odd,* $k \neq 2$ *and either* g *or* k *is not equal to* 3.

Proof. A primitive k-differential on a hyperelliptic genus g Riemann surface with a unique zero of order $2k(g-1)$ is equivalent to a primitive solution of (PA) of degree $n = k(g-1)$. Indeed, consider a solution of degree n of the Pell–Abel equation. According to point 3) of Remark 1, there exists a hyperelliptic Riemann surface M_∞ such that

$$n\infty_+ - n\infty_- \sim \mathcal{O}, \tag{23}$$

where $\mathcal{O}$ is the trivial bundle of M_∞. Moreover, by primitivity of the solution this equation is not satisfied for any $n' < n$. Since we know that

$$(g-1)\infty_+ + (g-1)\infty_- \sim K, \tag{24}$$

where K is the canonical bundle of M_∞, we obtain

$$2n \cdot \infty_+ = kK. \tag{25}$$

Therefore ∞_+ is the unique zero of a k-differential ξ. The fact that n is minimal for this property implies that ξ is a primitive k-differential in the locus $\Omega^k\mathcal{M}_g(2k(g-1))^{\mathrm{prim}}$.

Conversely, consider a primitive k-differential (M, ξ) in the hyperelliptic locus of the strata $\Omega^k\mathcal{M}_g(2k(g-1))^{\mathrm{prim}}$. The zero z of ξ satisfies (25). Now it suffices to subtract k times (24) from this equation to obtain (23). Recall that the degree of the solutions associated with the point z forms a semi-group generated by one element. Together with the primitivity of the k-differential this implies the primitivity of the solution associated with (23).

Hence, the components are in one-to-one correspondence with components of the primitive solutions of the Pell–Abel equation of degree $n = k(g-1)$. Note that $g > n - g - 1$ if and only if $k < (2g+1)/(g-1)$. For $g \geqslant 3$, this happens if and only if $k = 2$ or $k = g = 3$.

Since for $g = 2$ we obtain a bijection between the components of $\Omega^k\mathcal{M}_g(2k)^{\mathrm{prim}}$ and the components of the primitive solutions of the Pell–Abel equation of degree k, we obtain the result for genus 2 directly from Theorem 1.2.

https://doi.org/10.1112/S0010437X25007158 Published online by Cambridge University Press

So if $k=2$, we have $\min(g, 2(g-1)-g-1)=g$ and, using Theorem 1.2, we obtain that the number of connected components is equal to $[(g-1)/2]$. If $g=k=3$, the restriction of the stratum $\Omega^3\mathcal{M}_3(12)^{\mathrm{prim}}$ to the hyperelliptic locus is connected. If we are not in one of the previous cases, then the number of components is

$$\begin{cases} \left[\frac{g}{2}\right]+1 & \text{when } kg-k+g \text{ is odd,} \\ \left[\frac{g+1}{2}\right] & \text{when } kg-k+g \text{ is even.} \end{cases}$$

The second case occurs when both k and g are even, and the first case otherwise. This concludes the proof of Proposition 7.1. □

Since Riemann surfaces of genus 2 are hyperelliptic, this implies the first part of Corollary 4. Moreover, this shows that the parity invariant of [CG22, Theorem 1.2] classifies the connected components of $\Omega^k\mathcal{M}_2(2k)^{\mathrm{prim}}$. Recall that the parity invariant is given by the parity of the spin structure of the canonical cover associated with a k-differential (see [CG22, § 5] for a detailed discussion). We now relate the parity invariant to the degree partition invariant, proving the second part of the corollary.

Proposition 7.2. *Let $k \geqslant 5$ be an odd number. The component of $\Omega^k\mathcal{M}_2(2k)^{\mathrm{prim}}$ with odd, respectively even, parity corresponds to the component of invariant $(1,5)$, respectively $(3,3)$. Moreover, the component of $\Omega^k\mathcal{M}_2(2k)^{\mathrm{prim}}$ is odd if and only if there exists a Weierstraß point such that the difference between it and the zero of the k-differential is a k-torsion.*

The proof relies on the technology of the degenerations that were introduced in [BCG$^+$19] and studied in [CG22, § 2 and 3.2]. It is recommended that readers have some familiarity with these notions, but this is not necessary: we will only use the notion of twisted k-differentials which appear as the limit of k-differentials.

Proof. Let k be an odd integer $\geqslant 5$. Let $(M,\xi)\in\Omega^k\mathcal{M}_2(2k)$ be the primitive k-differential whose unique zero z is such that the graph associated with M (as explained in § 4) is linear. It is shown in the proof of [Gen22, Theorem 3] that there is a Weierstraß point $W\in M$ such that the difference $W-z$ is a k-torsion if and only if the linear graph has heights $(2,2,k-2)$. The degree partition invariant of this graph is $(1,5)$ (and of course W is the preimage of the unique $e\in\mathsf{E}^-$).

Let $(M,\xi)\in\Omega^k\mathcal{M}_2(2k)$ be a primitive k-differential of odd parity and denote its zero by z. It suffices to prove that there exists a Weierstraß point W such that $W-z$ is a k-torsion.

We start with a twisted k-differential (M_0,ξ_0) obtained by gluing the kth power of a holomorphic differential on a genus 1 Riemann surface (M_1,ω_1) to the pole of a k-differential (M_2,ξ_2) in $\Omega^k\mathcal{M}_2(2k,-2k)^{\mathrm{prim}}$ whose k-residue vanishes (see [CG22, Lemma 5.9] for the existence of such a k-differential). We denote by z the zero of ξ_2. We note that the Jacobian of the underlying singular curve M_0 is the product of the elliptic curves. This twisted k-differential (M_0,ξ_0) and its Jacobian are sketched in Figure 15.

This twisted differential is smoothable in the stratum $\Omega^k\mathcal{M}_2(2k)$. The limits of the Weierstraß points of any such smoothing are the 2-torsion points modulo the node N. Denote by W_1,W_2,W_3, respectively W_4,W_5,W_6, the 2-torsion points on M_1, respectively M_2. We consider the 2-torsion points on M_2. Let $v_1,v_2\in\mathbb{C}$ such that $M_2\sim\mathbb{C}/(\mathbb{Z}v_1\oplus\mathbb{Z}v_2)$, and suppose that the node is the image of $0\in\mathbb{C}$. The coordinates of z are $(n_1/2k, n_2/2k)$, where $\operatorname{pgcd}(n_1,n_2,2k)\in\{1,2\}$ is the rotation number of ξ_2 (see [CG22, Theorem 3.12]). Hence, the differences W_i-z are given by $((n_1-k\delta_1)/2k,(n_2-k\delta_2)/2k)$ with $(\delta_1,\delta_2)\in(\mathbb{Z}/2\mathbb{Z})^2\setminus\{(0,0)\}$. The orders of torsion of these

https://doi.org/10.1112/S0010437X25007158 Published online by Cambridge University Press

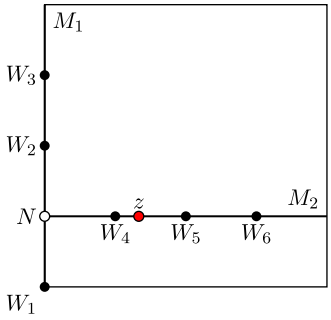


Figure 15 (colour online). The Jacobian of M_0.

differences are

$$\frac{2k}{\operatorname{pgcd}(n_1 - k\delta_1, n_2 - k\delta_2, 2k)}.$$

Suppose that the rotation number $\operatorname{pgcd}(n_1, n_2, 2k)$ of η_2 is 1. If both δ_i have the same parity as n_i, then both $n_i - k\delta_i$ are even. Hence there exists a 2-torsion point on M_2, given by $kz \in M_2$, such that its difference from z is k-torsion. Finally, [CG22, Lemma 5.6] shows that the parity of the k-differentials obtained by smoothing this twisted k-differential is odd. □

Acknowledgements

We thank Vincent Delecroix for the programming help and Victor Buchstaber for his constant interest in this topic. Various aspects of this work were discussed at the research seminars: Gonchar seminar on complex analysis, Steklov MI RAS; Graphs on surfaces and curves over arithmetic fields, Lomonosov Moscow State University; Seminar of International Lab for Cluster Geometry, HSE University; Novikov seminar on geometry, topology and math physics, Steklov MI RAS. The authors thank the organizers and all the participants of these seminars for fruitful discussions. Also we thank the anonymous referees of this paper for their valuable suggestions. Finally, our special thanks go to Jean-Pierre Serre who initiated our collaboration.

Conflicts of interest

None.

Financial support

The first author is supported by Moscow Center for Fundamental and Applied Math at INM RAS. The second author is supported by the Grant PAAPIT UNAM-DFG DA100124 'Conectividad y conectividad simple de los estratos' at INM RAS (agreement 075-15-2025-347).

Journal information

Compositio Mathematica is owned by the Foundation Compositio Mathematica and published by the London Mathematical Society in partnership with Cambridge University Press. All surplus income from the publication of *Compositio Mathematica* is returned to mathematics and higher education through the charitable activities of the Foundation, the London Mathematical Society and Cambridge University Press.

https://doi.org/10.1112/S0010437X25007158 Published online by Cambridge University Press

References

Abe26 N. Abel, *Ueber die integration der differential-formel* $\frac{\rho dx}{\sqrt{R}}$, *wenn* R *und* ρ *ganze functionen sind*, J. Reine Angew. Math. **1** (1826), 185–221, French translation in *Œuvres complètes de Niels Henrik Abel*, tome 1 (1881), pp. 104–144.

BCG+19 M. Bainbridge, D. Chen, Q. Gendron, S. Grushevsky and M. Möller, *Strata of k-differentials*, Algebr. Geom. **6** (2019), 196–233.

BCZ22 F. Barroero, L. Capuano and U. Zannier, *Betti maps, Pell equations in polynomials and almost-Belyi maps*, Forum Math. Sigma **10** (2022), e84.

BE01 E. Belokolos and V. Enolski, *Reduction of abelian functions and algebraically integrable systems. I*, J. Math. Sci. **106** (2001), 3395–3486.

Bir75 J. Birman, *Braids, links, and mapping class groups. Based on lecture notes by James Cannon*, Annals of Mathematics Studies, vol. 82 (Princeton University Press, Princeton, NJ, 1975).

Bog99 A. Bogatyrëv, *Effective computation of Chebyshev polynomials for several intervals*, Sb. Math. **190** (1999), 15–50, English translation in Mat. Sb. **190** (1999), 1571–1605.

Bog02 A. Bogatyrëv, *Effective approach to least deviation problems*, Sb. Math. **193** (2002), 1749–1769.

Bog03 A. Bogatyrëv, *A combinatorial description of a moduli space of curves and of extremal polynomials*, Sb. Math. **194** (2003), 1451–1473.

Bog12 A. Bogatyrëv, *Extremal polynomials and Riemann surfaces*, Springer Monographs in Mathematics (Springer, Berlin, 2012), translated from the Russian original (MTsNMO, Moskva, 2005).

Bog19 A. Bogatyrëv, *Combinatorial analysis of the period mapping: the topology of 2d fibres*, Sb. Math. **210** (2019), 1531–1562.

Bog23 A. Bogatyrëv, *Degeneration of a graph describing conformal structure*, Sb. Math. **214** (2023), 106–119.

BG23 A. Bogatyrëv and Q. Gendron, *Number of components of Pell–Abel equations with primitive solution of given degree*, Uspekhi Mat. Nauk **78** (2023), 209–210, English translation in Russian Math. Surveys **78** (2023), 208–210.

BZ13 V. Burskii and A. Zhedanov, *On Dirichlet, Poncelet and Abel problems*, Commun. Pure Appl. Anal. **12** (2013), 1587–1633.

Che48 N. Chebotarëv, *Theory of algebraic functions* (OGIZ, Moscow–Leningrad, 1948).

CG22 D. Chen and Q. Gendron, *Towards a classification of connected components of the strata of k-differentials*, Doc. Math. **27** (2022), 1031–1100.

DR19 V. Dragović and M. Radnović, *Periodic ellipsoidal billiard trajectories and extremal polynomials*, Commun. Math. Phys. **372** (2019), 183–211.

GG06 J.-M. Gambaudo and É. Ghys, *Braids and signatures*, Bull. Soc. Math. France **133** (2006), 541–579.

Gen22 Q. Gendron, *Équation de Pell–Abel et applications*, C. R. Math. Acad. Sci. Paris **360** (2022), 975–992.

GK10 S. Grushevsky and I. Krichever, *The universal Whitham hierarchy and the geometry of the moduli space of pointed Riemann surfaces*, in *Geometry of Riemann surfaces and their moduli spaces*, Surveys in Differential Geometry, vol. 14 (International Press, 2010), 111–129.

KZ96 A. Khovanskij and S. Zdravkovska, *Branched covers of* S^2 *and braid groups*, J. Knot Theory Ramifications **5** (1996), 55–75.

Kol20 J. Kollár, *Pell surfaces*, Acta Math. Hung. **160** (2020), 478–518.

Kon91 M. Kontsevich, *Intersection theory on the moduli space of curves*, Funct. Anal. Appl. **25** (1991), 123–129.

Kon92 M. Kontsevich, *Intersection theory on the moduli space of curves and the matrix Airy function*, Commun. Math. Phys. **147** (1992), 1–23.

KZ03 M. Kontsevich and A. Zorich, *Connected components of the moduli spaces of Abelian differentials with prescribed singularities*, Invent. Math. **153** (2003), 631–678.

LZ04 S. Lando and A. Zvonkin, *Graphs on surfaces and their applications*, Encyclopaedia of Mathematical Sciences, vol. 141 (Springer, Berlin, 2004).

https://doi.org/10.1112/S0010437X25007158 Published online by Cambridge University Press

LO08 F. Liu and B. Osserman, *The irreducibility of certain pure-cycle Hurwitz spaces*, Amer. J. Math. **130** (2008), 1687–1708.

Mal02 V. Malyshev, *The Abel equation*, St. Petersburg Math. J. **13** (2002), 893–938.

McM06 C. McMullen, *Teichmüller curves in genus two: Torsion divisors and ratios of sines*, Invent. Math. **165** (2006), 651–672.

MP18 R. Moschetti and G. P. Pirola, *Hurwitz spaces and liftings to the Valentiner group*, J. Pure Appl. Algebra **222** (2018), 19–38.

Mul22 S. Mullane, *Strata of differentials of the second kind, positivity and irreducibility of certain Hurwitz spaces*, Ann. Inst. Fourier (Grenoble) **72** (2022), 1379–1416.

Peh93 F. Peherstorfer, *Orthogonal and extremal polynomials on several intervals*, J. Comput. Appl. Math. **48** (1993), 187–205.

Pla14 V. Platonov, *Number-theoretic properties of hyperelliptic fields and the torsion problem in Jacobians of hyperelliptic curves over the rational number field*, Russian Math. Surveys **69** (2014), 1–34.

Rob64 R. Robinson, *Conjugate algebraic integers in real point sets*, Math. Z. **84** (1964), 415–427.

Ser19 J.-P. Serre, *Distribution asymptotique des valeurs propres des endomorphismes de frobenius d'après Abel, Chebyshev, Robinson,. . .*, in *Séminaire Bourbaki, vol. 2017/2018*, exposés 1136–1150 (Société Mathématique de France, 2019), 379–426.

SY92 M. Sodin and P. Yuditskij, *Functions least deviating from zero on closed subsets of the real axis*, Algebra i Analiz **4** (1992), 1–61, Engl. transl., St. Petersburg Math. J. **4** (1993), 201–249.

Str84 K. Strebel, *Quadratic differentials*, Ergebnisse der Mathematik und ihrer Grenzgebiete. 3. Folge, vol. 5 (Springer, Berlin, 1984).

Thu79 W. Thurston, *The geometry and topology of three-manifolds*, Encyclopaedia of Mathematical Sciences http://library.msri.org/books/gt3m/PDF/13.pdf (1979).

Vas95 V. Vassiliev, *Ramified integrals, singularities and lacunas*, Mathematics and Its Applications, Dordrecht, vol. 315 (Kluwer Academic Publishers, Dordrecht, 1995).

Waj96 B. Wajnryb, *Orbits of Hurwitz action for coverings of a sphere with two special fibers*, Indag. Math. (N.S.) **7** (1996), 549–558.

Zan14 U. Zannier, *Unlikely intersections and Pell's equations in polynomials*, in *Trends in contemporary mathematics* (Springer, Cham, 2014), 151–169.

Zol77 E. Zolotarev, *On the application of elliptic functions to questions of maxima and minima*, Zapiski Imperatorskoi Akademii Nauk, SPb **30** (1877), 1–71.

Andrei Bogatyrëv ab.bogatyrev@gmail.com
Marchuk Institute of Numerical Math of Russian Academy of Sciences, ul. Gubkina, 8, Moscow 119333, Russia
Lomonosov Moscow State University, Leninskie Gory, 1, Moscow 119991, Russia
HSE University, Pokrovskii bulvar, 11, Moscow 109028, Russia

Quentin Gendron quentin.gendron@im.unam.mx
Instituto de Matemáticas de la UNAM, Ciudad Universitaria, Coyoacán 04510, México

https://doi.org/10.1112/S0010437X25007158 Published online by Cambridge University Press